Optimization of Aqueous Chlorine Photochemistry for Enhanced Inactivation of Chlorine-resistant Microorganisms

Jenna E. Forsyth

A thesis
submitted in partial fulfillment of the
requirements for the degree of

Master of Science in Engineering

University of Washington

2012

Committee:
Michael C. Dodd
John S. Meschke
Douglas E. Latch

Program Authorized to Offer Degree:
Civil and Environmental Engineering

University of Washington

Abstract

Optimization of Aqueous Chlorine Photochemistry for Enhanced Inactivation of Chlorine-resistant Microorganisms

Jenna E. Forsyth

Chair of the Supervisory Committee:
Assistant Professor Michael C. Dodd
Department of Civil and Environmental Engineering

Bacillus subtilis spores, which are highly resistant to chlorine disinfection, have frequently been used as models for such chlorine-resistant, waterborne pathogens as *G. lamblia* and *C. parvum*. The goal of this research was to investigate the use of simulated sunlight to produce hydroxyl radical via HOCl/OCl$^-$ photolysis during free chlorine disinfection to synergistically enhance *B. subtilis* spore inactivation. Reactors were irradiated indoors using a Newport solar simulator equipped with a 450-W Xenon lamp (O$_3$ free) or outdoors with natural sunlight. The solar simulator emits light primarily at non-germicidal wavelengths between 300 and 400nm. At starting conditions, reactors contained phosphate buffer (0.01 M, pH 6-8) or natural NOM-containing water sampled from nearby municipal treatment facilities (pH 7.4), 10^4-10^5 CFU/ml *B. subtilis* spores, and *para*-chlorobenzoic acid (pCBA) as a hydroxyl radical probe. The inactivation of *B. subtilis* spores at 10, 25 (indoor) and 33 °C (outdoor) was monitored after adding between 1-8 mg L^{-1} as Cl$_2$ of free available chlorine (FAC) and either keeping reactors in the dark or exposing them to simulated or natural sunlight for a brief period of time. After removing irradiated reactors from the light source, continued inactivation by FAC was monitored in the dark. *B. subtilis* spores were enumerated using the spot titer culture assay method, allowing for at least 2-log$_{10}$-unit reductions to be measured in all cases. Inactivation of *B. subtilis* spores was modeled using the delayed Chick-Watson model. Inactivation was primarily characterized by pseudo-first order rate constants (*k,* in L(min-mg)$^{-1}$), lag phase length (in Ct

units), and Ct_{99} values. The Ct_{99} refers to the Ct (in (mg-min) L^{-1}) needed to achieve a 2-$\log_{10}$ (99%) reduction. To understand the effect of hydroxyl radical exposure on enhancement of inactivation by FAC, the rate enhancement factor (ratio of light:dark) and lag phase or Ct_{99} reduction factors (ratio of dark:light) were calculated. Neither simulated sunlight nor natural sunlight inactivated *B. subtilis* spores on their own. With FAC alone, inactivation efficiency was negatively related to pH and positively related to temperature. For phosphate-buffered solutions, pH was the most important determinant of the enhancement effect from irradiation with FAC: reducing Ct_{99} values more than two-fold at pH 8. Overall, the Ct_{99} reduction factor showed a positive linear relationship with pH that was independent of temperature (including 10, 25 and 33 °C data). In natural waters with low NOM levels, the enhancing effect of simulated solar radiation was only slightly lower than would be expected based on pH despite much slower dark inactivation with FAC only. The enhancing effect of irradiation is hypothesized to be due primarily to the generation of hydroxyl radical during FAC photolysis. Accordingly, when a hydroxyl radical scavenger, *tert*-butanol (50 mM), was added to FAC-containing reactors during irradiation, kinetics were reduced to the level observed with FAC alone. Previous studies have indicated that hydroxyl radical effectively destroys chlorine-recalcitrant components of the *B. subtilis* spore coat and/or cortex. Thus, in this system, initial attack by hydroxyl radical may make the spores more vulnerable to subsequent attack by free chlorine, resulting in a synergistic effect. These findings highlight the possibility of augmenting chlorination strategies for inactivation of otherwise chlorine-recalcitrant organisms through the use of low-energy photochemical energy sources (*i.e.*, sunlight, fluorescent lamps), as well as more energy-intensive germicidal UV light, in centralized and decentralized water treatment applications.

ACKNOWLEDGEMENTS

TABLE OF CONTENTS

LIST OF COMMONLY USED ABBREVIATIONS

Abbreviation	Item or Parameter
AAF	Atmospheric Attenuation Filter
ASTM	American Society for Testing and Materials
Ct	Product of disinfectant concentration and time (in (mg-min) L^{-1})
Ct_{99}	Ct value at 2 $\log_{10}$-units of inactivation
CFU	Colony Forming Units
DBP	Disinfection-by-product
DI	Deionized
DM	Dichroic Mirror
DPD	N-N-diethyl-p-phenylene diamine
FAC	Free Available Chlorine
Fluence	Radiative flux integrated over time
HAA	Haloacetic Acid
HOCl	Hypochlorous Acid
HO•	Hydroxyl Radical
HPLC	High Performance Liquid Chromatography
NOM	Natural Organic Matter
NTU	Nephelometric Turbidity Unit
OCl-	Hypochlorite ion
OD	Optical Density
PBS	Phosphate-buffered solution
pCBA	para-chlorobenzoic acid
PNA	p-Nitroanisole
Pyr	Pyridine
SODIS	Solar Disinfection
$SUVA_{254}$	Specific UV Absorbance at 254 nm
THM	Trihalomethane
UVA Light	320-400nm
UVB Light	280-320 nm
UVC Light	100-280 nm

LIST OF FIGURES

LIST OF TABLES

Table Number   **Page**

1. INTRODUCTION

1.1 Motivation

1.1.1 Brief History of Chlorine as a Disinfectant

Chlorine is the most common drinking water and wastewater disinfectant worldwide (*1*). Although initially introduced for continual use as a water disinfectant in Belgium in 1902, its first application in the U.S. was at a municipal water treatment plant in New Jersey in 1908 (*2*). Before long, chlorination became the most accepted water treatment method throughout the U.S., Europe, and the rest of the world. In developed countries, chlorination primarily occurs at centralized, municipal water treatment facilities, whereas in many developing countries that lack access to centralized water treatment, households or individuals are responsible for treating their own water, often with chlorine (*3*). Chlorine is simple to use and it is easy to scale operations from the individual level to large facilities serving thousands of individuals.

The benefits of chlorine to public health cannot be understated. In 20th century America, the introduction of chlorine-based water treatment is thought to have been partially responsible for the dramatic reduction in national typhoid rates by the 1940s (*4*). Chlorine has also reduced the burden of cholera epidemics, from that which occurred two centuries ago in London to recent epidemics in Haiti and sub-Saharan Africa (*5*). In addition to reducing the incidence of well-known diseases such as typhoid and cholera, improvements in drinking water quality from chlorine treatment have contributed to reductions in chronic diarrheal diseases. These diseases are a significant concern among those without access to safe water and may be responsible for almost 2.2 million deaths per year (*6*).

In addition to health benefits conferred by chlorine's general ability to eliminate waterborne pathogens, the United States Environmental Protection Agency (EPA) states that chlorine has the least expensive production and operating costs and longest history of use of any disinfectant (*7*). It is also possible to maintain a chlorine residual that provides long-term protection against re-

1

contamination. The World Health organization recommends a chlorine residual of 0.2-2 mg L^{-1} to protect public health (*8*).

However, chlorine has two main drawbacks related to public health: i) it is ineffective against chlorine-resistant pathogens such as *Cryptosporidium parvum*, and ii) it can react with organic matter naturally present in water to produce carcinogenic disinfectant-by-products (DBPs). In 1993, over 400,000 residents of Milwaukee fell ill due to deficiencies in chlorine-based water treatment (*9*). Researchers surmised that *C. parvum*, a highly chlorine-resistant pathogen, entered the water treatment plant from Lake Michigan waters and was inadequately removed by the combined treatment from chlorination, coagulation, and filtration. Although previous *C. parvum* outbreaks linked to water treatment failures had occurred in England, this was the first of such large magnitude in the U.S.

In response, the U.S. EPA and other regulatory bodies developed a series of standards to increase monitoring and treatment of chlorine-resistant pathogens like *C. parvum.* Expanding on the Surface Water Treatment Rule in 1989 that focused on increasing disinfection and filtration to remove *Legionella* and *Giardia*, the U.S. EPA initiated the Interim Enhanced Surface Water Treatment Rule in 1998 to address *C. parvum.* Additional rules included the Long Term 1 and Long Term 2 Enhanced Surface Water Treatment Rules in 2002 and 2003 that brought more attention to the subject, in addition to focusing on the concern of Disinfection By-Product (DBP) formation during chlorination. Additional regulations related to DBP formation included the Stage 1 and Stage 2 D/DBP rules (*10*).

Along with these regulations, municipal treatment facilities shifted from chlorine as a primary disinfectant to more cost- and energy-intensive UV, ozone (O_3), or filtration techniques followed by chlorine as a secondary disinfectant. Despite this shift, chlorine was still used in 97% of drinking water facilities in the U.S. as of 2000 (*11*).

Instead of shifting to other treatment techniques, this study focused on generating powerful oxidants from chlorine in solution via solar photolysis. This process could use pre-existing chlorination infrastructure in a novel way, be inexpensive, simple, and effective at inactivating

2

chlorine-resistant pathogens. Furthermore, the process could be much more favorable than alternative treatment techniques in terms of the time and energy required while minimizing the formation of carcinogenic DBPs.

1.2 Theory

1.2.1   Chlorine

1.2.1.1 Chlorine Speciation

Chlorine is commonly administered for water treatment as either molecular chlorine (Cl_2) or sodium hypochlorite (NaOCl). In solution, chlorine disproportionates into hypochlorous acid (HOCl) and its conjugate base, hypochlorite (OCl^-) (Equations 1-3). The combination of HOCl and OCl^- is commonly referred to as free available chlorine (FAC).

$$Cl_{2(g)} + H_2O \leftrightarrows HOCl + H^+ + Cl^- \quad (K\text{=}3.94 \text{ x } 10^{-4}) \, (12) \tag{1}$$

$$NaOCl + H_2O \leftrightarrows Na^+ + OH^- + HOCl \, (13) \tag{2}$$

$$HOCl \leftrightarrows OCl^- + H^+ \, (pKa\text{=}7.5 \text{ at } 25 \, ^\circ C) \, (14) \tag{3}$$
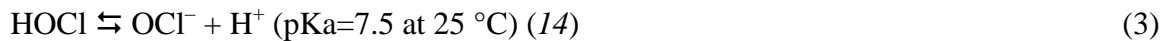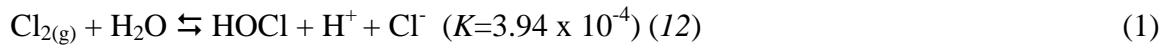
As shown in the above equations and Figure 1, solution pH influences FAC speciation. Above pH 9 (25 °C), OCl^- predominates. At pH 7.5 there are equal proportions of HOCl and OCl^-. Between pH 1 and 5, HOCl is the dominant species. And below pH 1, the proportion of Cl_2 reaches a maximum. At circumneutral pH, typical of drinking water, FAC is generally present as a combination of HOCl and OCl^- (Figure 1.1).

3
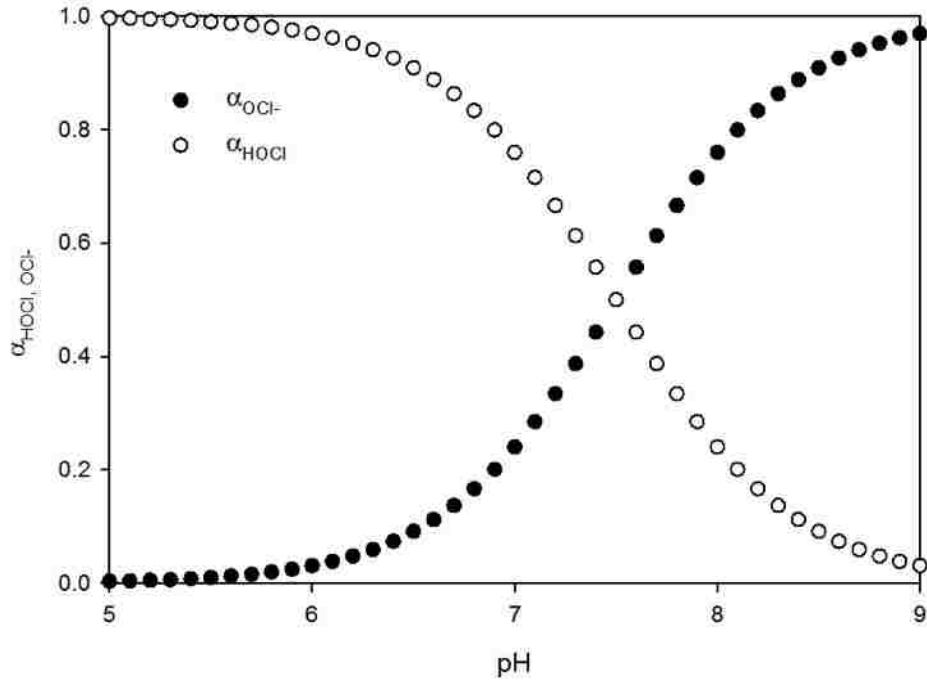
Figure 1.1: FAC speciation as HOCl and OCl⁻ as a function of pH at a chloride concentration of 0.3 mM.

1.2.1.2 Mechanism of Disinfection

Overall, FAC is considered to be a moderately effective disinfectant (*15*). The pH-dependent speciation of FAC is particularly important in the context of disinfection since HOCl and OCl⁻ do not possess equivalent disinfection capabilities. HOCl is a considerably stronger disinfectant than OCl⁻ (*1*). Thus, increasing pH results in less effectiveness due to an increasing contribution from OCl⁻, while decreasing pH results in greater effectiveness due to HOCl.

Often used as an indicator of biocidal activity, the reduction potential of HOCl is approximately 1.48 volts at pH 8 and 20 °C (*16*). Although less than the reduction potential of O_3 and chlorine dioxide (ClO_2), FAC's reduction potential is greater than that of chloramine (NH_2Cl) (*17*). Similar to NH_2Cl, however, FAC provides an advantageous stable residual.

4

The effectiveness of FAC as a disinfectant exhibits a positive relationship with regard to temperature. As explained by the van't Hoff-Arrhenius equation and FAC's relatively high activation energy, increasing temperature increases FAC's reactivity (*18*).

FAC's mechanism of disinfection has been the focus of considerable research. FAC is most reactive toward proteins and only moderately reactive toward nucleic acids and lipids, and less reactive toward polysaccharides. FAC is selective, targeting specific groups, such as sulfhydryl groups on proteins or other biomolecules (*19*). FAC can disrupt cellular function by oxidizing metabolic proteins or nucleic acids or oxidizing cell membrane constituents that result in irreparable morphological changes to the microorganism (*20*). FAC is thought to inactivate spores by oxidizing inner membrane proteins, which increases membrane permeability and susceptibility to subsequent oxidative attack (*21*).

1.2.2 Chlorine-resistant Microorganisms

1.2.2.1 General Characteristics

Despite FAC's general effectiveness, chlorine is not as effective against "chlorine-resistant" microorganisms. Chlorine-resistance is a function of the characteristics of a microorganism and its environment. While viruses are generally susceptible to chlorination, they may become difficult to disinfect if adhered to larger particles (*22*). Overall, vegetative bacterial cells are considered susceptible to FAC. Certain bacteria form spores (*Bacillus* or *Clostridium* spp.) and are much more resistant to chlorination as spores than as vegetative cells (*23*). Some protozoa, notably the pathogenic *Cryptosporidium parvum*, are very chlorine-resistant, requiring impractically high concentrations of chlorine or residence times in order to achieve adequate inactivation (*24*).

Many researchers have investigated the behavior of chlorine-resistant, yet non-pathogenic, *Bacillus subtilis* spores as potential surrogates for *C. parvum* (*25*, *26, 27*). While *B. subtilis* spores are less chlorine-resistant than *C. parvum* and behave differently when exposed to oxidants (*28*), they have been shown to be more resistant than *G. lamblia* to chlorination (*29*). Furthermore, the breadth of information accrued from years of research make *B. subtilis* spores a good subject of further disinfection studies comparing FAC resistance and alternative oxidative processes.

Unfavorable environmental conditions trigger the transformation from vegetative cells to spores. *B. subtilis* spores respond to environmental cues when conditions improve by germinating as vegetative cells. The transformation from the metabolically active vegetative cell to the resilient spore gave spore-forming bacteria an evolutionary advantage, enabling them to withstand severe conditions for considerable lengths of time. There have been accounts of million-year old viable spores preserved in lake sediments (*21*).

The spore's ability to survive is related to its anatomy. *B. subtilis* spores possess a thick proteinaceous coat composed of as many as 25 different cross-linked proteins that offer considerable protection against heat and chemical treatment (*30, 31*). Recent research has indicated that spore chromosomes are attached to small acid-soluble proteins (SASPs) that offer some protection against UV damage, heat, and some chemicals (*31, 32*). Furthermore, spores are capable of repairing damaged DNA during germination (*33, 31*).

1.2.3   Hydroxyl Radical as a Disinfectant

1.2.3.1 Photolytic Generation and Chemistry

Hydroxyl radical (HO$^{\bullet}$) is highly unstable due its single electron deficiency. HO$^{\bullet}$ as commonly been generated in order to destroy organic and inorganic chemical contaminants in waters. Photochemical and Advanced Oxidative Processes (AOPs) have been developed to generate HO$^{\bullet}$

including O_3/H_2O_2 reactions, photo-Fenton reactions involving H_2O_2 and Fe^{2+}, and the photolysis of H_2O_2 or NO_3^-/NO_2^- (*34, 35, 36*). FAC can also be photolyzed to generate $HO^{\bullet}$(*37*).

Using FAC as a photochemical source of $HO^{\bullet}$ has been scarcely studied for practical applications, although the photochemical processes are well known (Eq. 4-7). Upon photo-excitation with light of $\lambda < 400$ nm, HOCl and OCl^- are homolytically cleaved to form $HO^{\bullet}$ according to the following series of reactions:

$$HOCl + h\nu \rightarrow HO^{\bullet} + Cl^{\bullet} \qquad \eta_{HO_{\bullet},255nm} = 0.9, \eta_{HO_{\bullet},sunlight} = 0.7 \qquad (4a)$$

$$OCl^- + h\nu \rightarrow O^{\bullet-} + Cl^{\bullet} \qquad \eta_{O_{\bullet}-,255nm} = 0.1, \eta_{O_{\bullet}-,sunlight} = 0.1 \qquad (4b)$$

$$O^{\bullet-} + H_2O \leftrightarrows HO^{\bullet} + OH^- \qquad K_2 = 1.4 \times 10^{-4} \qquad (5)$$

$$Cl^{\bullet} + H_2O \leftrightarrows HOCl^{\bullet-} + H^+ \qquad K_3 = (1.4 \pm 0.53) \times 10^{-7} \qquad (6)$$

$$HOCl^{\bullet-} \leftrightarrows HO^{\bullet} + Cl^- \qquad K_4 = 1.4 \pm 0.26 \qquad (7)$$
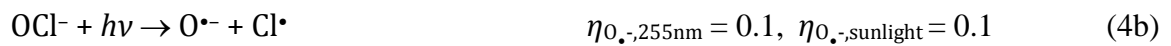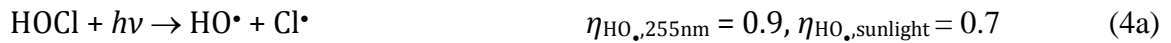
In the above, $\eta_{HO_{\bullet}}$ represents a $HO^{\bullet}$ yield factor equal to $\Delta[HO^{\bullet}]_{generated}/ \Delta[FAC]_{photolyzed}$, $\eta_{O_{\bullet}-}$ represents a $O^{\bullet-}$ yield factor equal to $\Delta[O^{\bullet-}]_{generated}/\Delta[FAC]_{photolyzed}$, and "sunlight" refers to wavelengths of 300 nm $< \lambda < 400$ nm.

In addition to $HO^{\bullet}$ formation, the photooxidant, $Cl^{\bullet}$, is generated during FAC photolysis. However, at circumneutral pH, and in the presence of low Cl^- concentrations, the $Cl^{\bullet}$ generated in reactions 4a and 4b would react predominantly with H_2O to form $HOCl^{\bullet-}$ (Eq. 6). Subsequently, $HOCl^{\bullet-}$ would decay to yield additional $HO^{\bullet}$ (Eq. 7). Therefore, given pH and Cl^- conditions typical of drinking water, the majority of $Cl^{\bullet}$ generated by FAC photolysis would also be converted to $HO^{\bullet}$ (*37*).

The efficiency with which FAC is converted to $HO^{\bullet}$ is described by the $HO^{\bullet}$ yield factor, $\eta_{HO_{\bullet}}$, and is inversely related to pH. As demonstrated by 4a and 4b, the solar spectrum $HO^{\bullet}$ yield factor is seven times greater for HOCl ($\eta_{HO_{\bullet}} = 0.7$) than OCl^- ($\eta_{O_{\bullet}-} = 0.1$), indicating greater efficiency at lower pH.

www.manaraa.com

While the efficiency of solar FAC photolysis increases with decreasing pH, the opposite is true for the solar photolysis rate, which increases with increasing pH. The rate of FAC photolysis is faster for OCl⁻ than HOCl since OCl⁻ absorbs more light at solar wavelengths (Figure 2). Similarly, Nowell and Hoigné (1992) (*38*) reported the pseudo-first-order rate constant of solar photolysis as 2×10^{-4} s⁻¹ for HOCl and 1.2×10^{-3} s⁻¹ for OCl⁻. As demonstrated by Figure 1.2 and by taking into account the spectral rate of light absorption and molar absorptivity coefficients of HOCl and OCl⁻, as well as the irradiance intensity of sunlight, the optimal solar wavelength for photolysis of HOCl and OCl⁻ would be 330 nm (*38*). In contrast, at a monochromatic wavelength of 253.7 nm (commonly used in UV disinfection applications) the HOCl and OCl⁻ absorption spectra intersect, indicating that the rate of FAC photolysis would be pH-independent near that wavelength.
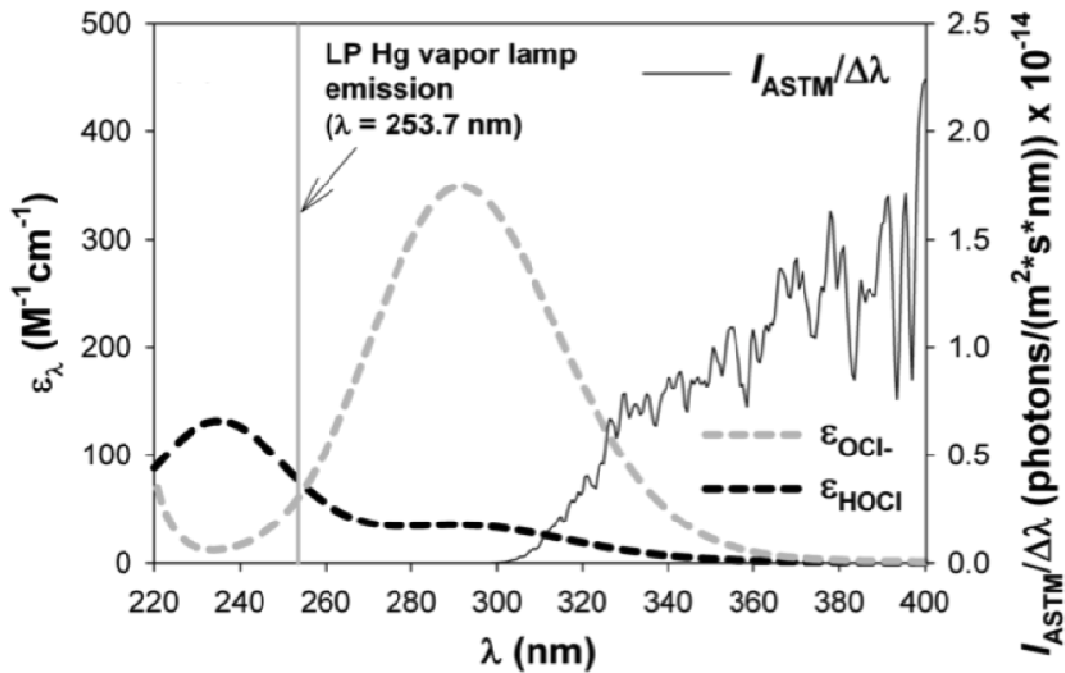
Figure 1.2: FAC molar absorptivity (ε) and solar irradiance versus wavelength. Note at λ=253.7 HOCl and OCl⁻ have equal absorptivities. I_ASTM refers to the irradiance of the standard Terrestrial Reference Spectra reported by the American Society for Testing and Materials (ASTM).

8

1.2.3.2 Mechanism of Disinfection

Disinfection by HO$^\bullet$ is primarily controlled by oxidation of cell constituents and diffusion into the cell (*39*). HO$^\bullet$ is a highly electrophilic and powerful oxidant with an oxidative potential almost twice that of FAC (2.70 V versus 1.36 V for FAC) (*40*). Unlike FAC, HO$^\bullet$ is extremely short-lived due to its high reactivity toward organic and inorganic compounds. As a result, the half-life of HO$^\bullet$ is only 10^{-9} seconds (*41*). HO$^\bullet$ is capable of effectively oxidizing all classes of biomolecules present in microorganisms including nucleic acids, protein, lipids, and polysaccharides (*42, 43, 44*). Since it is highly reactive, HO$^\bullet$ attacks whatever it comes in contact with first, most often the outer cell membrane and wall constituents (*42*). This destruction of cell membrane or wall structures can impede normal function, rendering the cell non-viable (*21*). In this way, HO$^\bullet$ may oxidize the highly protective exterior of chlorine-resistant microorganisms such as *B. subtilis* and *C. parvum* (*43*).

The secondary proposed mechanism of disinfection by HO$^\bullet$ is by diffusion into a cell followed by oxidation of cellular constituents (i.e., amino acids of critical enzymes). Reacting with intracellular constituents could inhibit normal cell processes including protein synthesis and transcription or translation of DNA, among others. Diffusion into a cell is controlled by charge, molecular weight and a disinfectant's half-life (*39*). Disinfection by HO$^\bullet$ is thought to be more diffusion-limited as the surface area-to-volume ratio of microorganisms increases, leading to faster rates of inactivation for viruses compared to bacterial cells (*45*).

1.2.4 The Ct Concept

For regulatory and comparative purposes, an oxidant's effectiveness as a disinfectant can be assessed by comparing the Ct value necessary in order to achieve a certain level of $\log_{10}$ inactivation where one $\log_{10}$-unit of inactivation refers to a 90% reduction in the number of viable microorganisms (Eq. 8).

$$Ct = 2.303/k \times (\# \text{ logs of removal}) \tag{8}$$

9

In the above equation, C is the concentration of the disinfectant, t is exposure time, and k is the pseudo-first order inactivation rate constant.

The Ct value is the integrated concentration of oxidant over the oxidant's residence time in the water, modeled as an ideal plug-flow reactor (PFR). The Ct value can be determined by the following equation (Eq. 9):

$$Ct = \int_0^t C_{(t)} dt \qquad (9)$$

Ct values have been reported for FAC at varying pH and temperature. At pH 8, 20 °C, Cho and Yoon (2006) (*40*) showed that FAC Ct values necessary to achieve 2 $\log_{10}$-units of inactivation (Ct$_{99}$ value achieving a 99% reduction in microorganisms) varied by five orders of magnitude when comparing the gram-negative bacterium, *E. coli*, to the more chlorine-resistant *B. subtilis* spores and highly resistant *C. parvum*. The specific Ct$_{99}$ values were 1.3 x 10^{-1} (mg-min) L^{-1} for *E. coli*, 450 (mg-min) L^{-1} for *B. subtilis* spores and 4,200 (mg-min) L^{-1} for *C. parvum*. Meanwhile, HO$^\bullet$ Ct$_{99}$ exposure values were substantially less than for FAC and much more similar to each other, ranging from 1.5 x 10^{-5} (mg-min) L^{-1} for *E. coli*, 8.2 x 10^{-5} (mg-min) L^{-1} for *B. subtilis* spores, and 9.3 x 10^{-5} (mg-min) L^{-1} for *C. parvum* (*40*).

1.2.5 UV and Solar Disinfection

Germicidal UV light is becoming a more common component of the municipal drinking water treatment process due to its effectiveness against many chlorine-resistant microorganisms. Unlike chemical disinfection, inactivation by UV light depends upon radiant energy (inversely related to wavelength), the absorption spectra of target molecules, and the susceptibility of target molecules to damage following light absorption. Germicidal UVC light is highly effective at inactivating *B. subtilis* spores. DNA and RNA readily absorb light in this range, yielding thymine dimers as a consequence, which may result in mutations or limit a cell's ability to replicate (*46*). However, UV disinfection requires the use of expensive energy-intensive UV lamps and does not provide a protective residual like FAC.

10

In decentralized settings, natural sunlight has also been used to disinfect water, although this typically requires long exposure periods. Such solar disinfection, known as SODIS, is commonly employed at the household level in developing countries. SODIS involves exposing small volumes of water of low turbidity (< 30 NTU) to sunlight over at least six hours (47). Researchers hypothesize that SODIS disinfects by a combination of the UVA/UVB radiation from sunlight and increasing water temperature due to infrared radiation. However, for both spores and protozoa, the process is extremely slow. The spore coat and cortex of *B. subtilis* may provide some resistance to damage by solar wavelengths of light, explaining its resistance to SODIS (30). Researchers have had limited success inactivating *B. subtilis* using SODIS. Boyle et al. (2008) (48) reported only 1.3 $\log_{10}$-units reduction in *B. subtilis* spores after 16 full hours of sunlight over 2 days (dose of 79.9 MJ m^{-2}). Malato et al. (2009) (49) concluded that SODIS is ineffective and therefore not practical for *B. subtilis* spores.

Recently, the notion of enhancing SODIS by adding H_2O_2 to generate low levels of HO• s has gained traction. Fisher et al. (2008) (50) witnessed a linear increase in inactivation of *E. coli* with increasing concentrations of H_2O_2 between 0 and 500 μM. Following six hours of exposure to sunlight with 200 μM H_2O_2 added, the researchers found more than 2 $\log_{10}$-units of inactivation of *E. coli* but no inactivation in sunlight alone over that same 6-hour period (50).

The disadvantages of both SODIS and enhanced SODIS include not only time, but also the lack of a residual protection against recontamination. Researchers have reported microbial re-growth and the potential for re-contamination as a limitation of SODIS (51). Therefore, the proposed system, generating HO$^{\bullet}$ from FAC using solar light, could provide added benefit in this setting.

1.2.6 Combining Disinfectants

While many researchers have confirmed that HO$^{\bullet}$ can effectively remove organic contaminants or DBPs from water (52, 53, 54, 55, 56), few have investigated its capacity to inactivate microorganisms. Of those researchers studying HO$^{\bullet}$'s biocidal activity, most have examined sequential application of HO$^{\bullet}$ or other short-lived advanced oxidants such as O_3, followed by application of longer-lived FAC or NH_2Cl as a secondary disinfectant and in order to achieve a

11

protective residual. Researchers have examined pre-treatment with $HO^{\bullet}$, ClO_2, or UV followed by FAC as secondary disinfectant. Enhanced inactivation was observed with $HO^{\bullet}$, O_3 and ClO_2 followed by FAC but not with UV. The nature of the synergistic effect was either to shorten the lag phase, speed up the rate of inactivation, or both for *C. parvum* and *B. subtilis* spores (*57*, *40*). Both of these effects, a reduction in lag phase and an increase in inactivation rate, function to reduce overall time required for disinfection. Since the magnitude of these effects may not be equal, Cho et al. (2006) (*40*) developed a parameter known as the percent synergistic effect to indicate the additional log inactivation achieved via sequential disinfectant application compared to individual application. For example, in the case of a UV/H_2O_2 system administered to generate $HO^{\bullet}$ followed by FAC, there was a 65% synergistic effect, resulting in approximately 3.3 $\log_{10}$-units of inactivation when 2 $\log_{10}$-units would be expected (*58*).

1.3 Objectives

With an understanding of the many strengths and weakness of FAC as a disinfectant, the broad objective of this investigation was to investigate simple, practical and low-cost solutions to enhance chlorine-based inactivation of the model chlorine-resistant microorganism, *Bacillus subtilis* spores.

Under the broad objective, the primary aim was to investigate the process of photochemically activating chlorine to $HO^{\bullet}$ during solar photolysis to disinfect *B. subtilis* spores. Through the photolysis of FAC to generate $HO^{\bullet}$, the intention was to maintain the benefits of chlorine by providing a long-term residual, but also to achieve greater inactivation of *B. subtilis* spores in a shorter period of time than would be possible with FAC alone.

In order to optimize the process, it is important to understand the effect of the following variables on *B. subtilis* spore inactivation: pH, temperature, FAC concentrations, irradiation time, presence of organic matter (comparing natural water and phosphate-buffered solutions), and real versus simulated sunlight. Optimization generally refers to the process of improving efficiency by maximizing outputs with minimal inputs. In this case, it refers to simplifying the steps

involved and minimizing the time required to achieve a target level of disinfection and thereby reducing associated costs, from equipment to human resources.

2. MATERIALS AND METHODS

2.1 Standards and Reagents

De-ionized water with resistivity ≥ 18.2 M$\Omega\bullet$cm obtained from a Millipore Milli-Q Ultrapure system was used for the preparation of all experimental solutions unless otherwise noted. NaOCl as 5% FAC was purchased from JT Baker and standardized spectrophotometrically at $\lambda = 292$ nm, using $\varepsilon_{292nm,OCl^-} = 350$ M^{-1}cm^{-1} (*59*). Spectrophotometric measurements were made on a Perkin Elmer Lambda-18 UV/Vis Spectrophotometer. N-N-diethyl-p-phenylenediamine (DPD) was purchased from Fluka. DPD stock solutions and phosphate buffers were prepared according to Standard Methods (*60*). DPD stock was stored in the dark at 4 °C and replaced every three weeks or until a pink color appeared. Sodium thiosulfate, $Na_2S_2O_3$ (Fisher Scientific) stocks were prepared and stored in amber vials at 4 °C. The solution was replaced every three weeks. Tert-butanol (t-BuOH) was purchased from Sigma Aldrich (>99.7% purity) and stocks were prepared with glass syringes for improved accuracy ($\rho = 0.789$ g/mL). *p*-chlorobenzoic acid (pCBA) was purchased from Sigma Aldrich. Working stocks of 100μM pCBA were dissolved in 10mM sodium hydroxide (NaOH) and adjusted to circumneutral pH with 1 M phosphoric acid. For actinometry, *p*-nitroanisole (PNA) was purchased from Sigma Aldrich, with 97% purity. PNA was prepared in a 10 mM working stock solution, dissolved in acetonitrile. Pyridine (pyr) was purchased from JT Baker, with ACS-grade purity. Difco^{TM} Nutrient Broth, BBL^{TM} Nutrient Agar, and BBL^{TM} AK Agar #2 (Sporulating Agar) were purchased from the Becton, Dickson and Company (BD). All media was prepared according to the manufacturer's protocol including an autoclave cycle of 15 minutes at 121 °C for sterilization.

Buffers of varying pH were prepared with sodium phosphate salts (mono- and di-basic, disodium hydrogen orthophosphate and sodium dihydrogen orthophosphate) purchased from Sigma Aldrich with 99% purity. Phosphate-buffered-saline (PBS) for storage of vegetative and spore cells was prepared according to Sambrook et al. (2001) (*61*) using NaCl, KCl, Na_2HPO_4, KH_2PO_4 and adjusted to pH 7.4 with HCl. pH adjustments were made using a Thermo Scientific Orion 5 Star instrument. The pH meter was calibrated prior to each use. Phosphate buffers were

14

autoclaved at 121 °C for 15 minutes to ensure sterile conditions. Other reagents were sterilized using 0.22 μm filters (Fisherbrand MCE LOT# R9EN99100).

Untreated drinking water was obtained from two water treatment facilities in the Seattle area: i) The City of Marysville Stillaguamish Water Treatment Plant where the source water is from the Stillaguamish River; and ii) The Cedar Water Treatment Plant where the source water is the Chester Morse Reservoir. At the Marysville Stillaguamish Water Treatment Plant, the raw water is filtered and then FAC is added. For experimental purposes, samples were taken following ultrafiltration. At the Cedar Water Treatment Plant, the raw water is treated with ozone, UV, and then FAC is added. Samples from the Cedar Water Treatment plant were taken as raw water. These water samples were filter sterilized to remove any potential microbial contamination without altering the native chemical characteristics of the water (0.20 µm Thermo Scientific Nalgene Disposable Filter Unit, Lot #: 1063958).

2.2 *Bacillus subtilis* Spore Stock Preparation

2.2.1 Vegetative Cell Growth

Stocks of *B. subtilis* were prepared under sterile conditions using aseptic techniques performed in a Biosafety Level 2 hood (BSL-2). Freeze-dried *B. subtilis* (ATCC 6633) cells were inoculated in an Erlenmeyer flask containing nutrient broth to revive the vegetative cells. The Erlenmeyer flask was loosely capped to maintain aerobic conditions and incubated at 37 °Celsius at 150 shakes per minute in a benchtop shaking incubator. Incubation continued for approximately 30 hours or until the solution reached peak optical density (OD). The peak OD was determined by aseptically transferring 3 mL of solution to a disposable cuvette and reading the peak absorbance periodically throughout incubation, using a Hach DR 4000 UV-Vis Spectrophotometer ($190 < \lambda > 1100$ nm). After 30 hours of incubation, a peak OD of 0.5 at 600 nm was achieved, at the point when growth shifted from the lag to the exponential phase but well before reaching the stationary phase.

2.2.2 Sporulation

After achieving this degree of vegetative cell growth, the cells were concentrated by centrifuging at 3,500 G for 5 minutes, pouring off the supernatant, and resuspending the pellet in smaller volumes of sterile water. In order for sporulation to occur, the cells must be deprived of nutrients or face harsh conditions. To this end, 100- and 150-mm diameter petri dishes were prepared containing AK#2 sporulating agar which is formulated to induce sporulation in *Bacillus subtilis* cells. The concentrated vegetative cell solution was dispensed in aliquots of 0.2-0.5 mL on to each AK#2 petri dish and spread using a disposable cell spreader. Petri dishes were incubated at 37 °C for 5-7 days.

2.2.3 Spore Harvesting, Storage, and Purification

Following incubation, the AK#2 agar dishes were brought to room temperature. Small volumes of PBS were added to the dishes to loosen the spores for simple harvesting. Using a cell scraper and a 10 mL pipette with a Drummond Pipette Aid, spores were lifted from the agar and transferred to a conical tube.

Spore purification involved the repetition of many centrifugation steps. Spores were centrifuged three times at 10,000 G for 10 minutes. Each time, the supernatant was discarded and the pellet was re-suspended in sterile water. Next, spores were centrifuged at 20,000 G for 20 minutes, discarding the supernatant and re-suspending pellet in water. This step was repeated numerous times until the pellet possessed two layers: a thin lightly colored layer (vegetative cells) resting on a thicker darker colored layer (spore cells). Eventually, the upper layer sloughed off leaving a uniform darkly colored pellet of spores.

Spore and vegetative cell heat resistance was determined by conducting a heat treatment curve. Separate microcentrifuge tubes (1.5 mL) containing spore cells and vegetative cells were heated using a VWR brand digital heat block (accuracy ± 0.1 °C) at 70 °C and sampled at 1, 5, 10, and 20 minutes. Cell viability was assessed by the spot-titer method (description below). The purity of the spore stock was determined by observing any changes in cell counts attributable to

16

vegetative cell die-off. This also allowed for the determination of the optimal heating time to maintain spore stock purity for experimentation purposes by killing vegetative cells but not spores.

Spores were stored in sterile water at 4 °C and purified by centrifugation every 3 weeks. Prior to each experiment, spores were purified by heat treatment at 70 °C for 15 minutes in order to eliminate any vegetative cells. A single spore stock was used for all experiments due to potential variability in response of spore stocks resulting from even the slightest differences in sporulation, preparation, or storage (*39*).

2.3 *Bacillus subtilis* Cell Viability Assay

Spores were serially diluted (1:10) using PBS to yield dilutions spanning up to seven orders of magnitude. Spore viability was quantified via the spot-titer culture assay method (*62*). Eight replicate 10 µL droplets of three dilutions were dispensed onto 100-mm petri dishes (*i.e.,* Figure 2.1). The spots were left to absorb into the top layer of agar before placing in an incubator at 37 °C. After 15 hours of growth, 24 "spots" each containing between 1-100 colonies became visible. Colonies were counted immediately. This approach has been found to yield results statistically equivalent to those obtained by traditional spread plating as demonstrated by analysis of variance (ANOVA) and χ^2 (*62*). Additional advantages of the spot-titer method over spread plating include: i) time-savings since it is quicker to dispense droplets than to spread over a plate and it is quicker to count colonies in distinct spots than colonies spanning the surface area of an entire plate; and ii) cost- and resource-savings since an entire serial dilution series including replicates requires only one plate. Thus, analyses of large experiments were performed more quickly, more affordably, and with greater replicability than would have been possible with traditional spread plating methods.
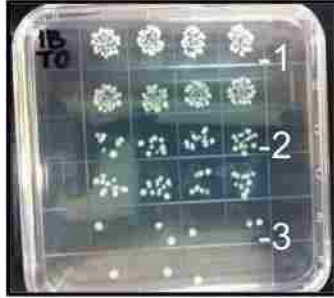
Figure 2.1: Example B. subtilis spot titer plate with 10^{-1}, 10^{-2}, and 10^{-3} sample dilutions plated.

2.4 Irradiation System, Radiometry, and Actinometry

For indoor bench-top experiments, solar radiation was simulated using a 450-W Xe arc lamp equipped with a focusing collimator (2"), atmospheric attenuation filter to exclude $\lambda < 300$ nm, and a dichroic mirror to dissipate infrared-generated heat (Figure 2.2) (Newport-Oriel Model 66924 arc lamp; Stratford, CT). The resulting radiation was restricted to UVA and some UVB with wavelengths between 300 and 400 nm. Spectral irradiance measurements for both indoor and outdoor experiments were obtained regularly using an Ocean Optics USB2000+spectroradiometer to ensure uniformity of lamp output.

Figure 2.2: Newport Solar Simulator lamp output configuration showing the dichroic mirror that absorbs infrared wavelengths and reflects other light at a right angle (atmospheric attenuation filter, AAF, not shown). Images obtained from the manufacturer.

Dilute solution actinometry was used for measurement of the *in situ* fluence rate during irradiation experiments. The *p*-Nitroanisole (PNA)/pyridine (PYR) system, developed for solar actinometric measurements by Dulin and Mill (1982) (*63*) was used. Fluence rates were

measured by PNA/PYR actinometry for both the simulated solar lamp and the rooftop experiments. Actinometry conditions were selected to approximate the absorptive characteristics of the spore inactivation systems. To achieve this, 40 and 25 mL actinometric solutions containing 50 μM PNA and 10 mM pyridine were prepared for indoor and outdoor experiments, respectively. In order to represent the experimental spore inactivation systems, actinometric solutions were prepared in the same 60 mL crystallization dishes as used for disinfection experiments under indoor simulated sunlight and in the same 30 mL quartz tubes as used for disinfection under outdoor natural sunlight. Actinometric solutions were kept in the dark until the start of the experiment, after which they were exposed to light over the same experimental time as the spore inactivation systems. The crystallization dishes used for indoor experiments had an inner diameter of 4.8 cm and depth of 2.2 cm with 40 mL solution volume. The quartz tubes for outdoor experiments were measured to have an inner diameter of 2 cm and depth of 12.5 cm with 25 mL solution volume.

2.5 Experimental Procedure

2.5.1 Simulated Sunlight: Indoor Bench-scale

Prior to each experiment, a Free Available Chlorine standard curve was developed using the N-N-diethyl-p-phenylenediamine (DPD) colorimetric method (description below) with an R-squared value of at least 99%. Additionally, *B. subtilis* spores were heat treated before every experiment at 70° C for 15 minutes to ensure spore purity.

Crystallization dishes (60 mL reactors) were filled with 40 mL 10 mM sodium phosphate buffer for pH regulation (from 6-9 at single unit intervals), 1uM pCBA to quantify HO$^{\bullet}$ exposure, and spiked with *B. subtilis* spores to target initial concentrations of 10^4-10^5 colony forming units per mL (CFU mL^{-1}) within the reactors. Depending on the experimental set-up, Free Available Chlorine (FAC) as Cl$_2$ was added at t=0. Initial chlorine concentrations varied between 1 and 8 (mg L^{-1}). Throughout the experiments, all reactors were covered with 1.5-mm thick quartz discs.

Dark reactors were placed in a covered container and constantly stirred using a 2Mag®
MixDrive15 multi-position stir plate (Figure 2.3a). Irradiated reactors were placed in the
Newport solar simulator and constantly stirred with a single-stir plate. After a defined period of
irradiation, irradiated reactors were placed in the covered container to continue reacting under
dark conditions. All reactors were stirred at 250 rpm. The temperature of all reactors was
regulated using a recirculating constant temperature bath. The temperature was set at 25 or 10°
C.
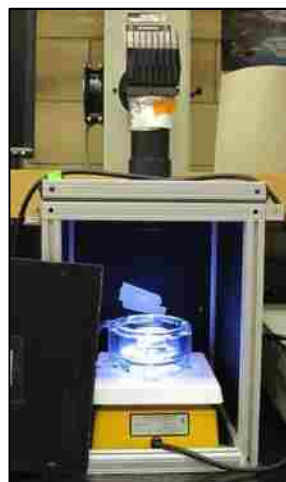
*Figure 2.3: Indoor reactor set-up using the multi-position stir plate in a temperature-controlled
bath (left) and the Newport Solar Simulator with a temperature-regulating bath and single
position stir plate (right).*

At pre-defined times throughout the experiments, paired sample volumes were collected
simultaneously for analysis of chlorine, pCBA, and spore concentrations. Specifically, one
volume was added immediately to a sample vessel pre-spiked with $Na_2S_2O_3$ to remove any
residual FAC and stored at 4° C for subsequent measurement of spore viability and pCBA
concentration. The second volume was added immediately to a sample vessel containing DPD
reagent to allow for colorimetric measurement of residual FAC. pCBA concentration was
determined by the method described in section 2.6 below and spore viability was quantified by
the spot-titer technique described above.

Several conditions were tested at pH 6, 7, and 8 and 10 and 25° C in triplicate:
1) Continuous irradiation with FAC
2) Continuous irradiation without FAC (light control)

20

3) Brief irradiation of FAC-containing solutions followed by dark FAC exposure
4) No irradiation (dark conditions) with FAC
5) Dark conditions without FAC (dark control)

The length of irradiation was calculated using FAC half-lives and HO• yields in order to target a level of HO• exposure (or mg L^{-1} FAC photolyzed). In order to confirm that any enhancements in inactivation observed in irradiated reactors were attributable to HO• exposure, irradiated reactor solutions identical to condition number one above were amended in selected experiments with 50 mM tert-butanol as a HO• scavenger (*64*).

2.5.2 Natural Sunlight: Outdoor

Outdoor experiments followed the same pre-experiment spore purification procedures as in the indoor experiments, in addition to chlorine photolysis measurements. Immediately before starting an outdoor experiment, chlorine photolysis rates under natural sunlight were measured in order to select optimal irradiation time, dark time, and sampling times.

Outdoor experiments were conducted on the roof of More Hall at the University of Washington in Seattle, WA (latitude 47°36'35''N) on a clear day at 12:00 PM with no cloud-cover. Although the general experimental design was similar to that used in indoor experiments, the outdoor conditions required the use of different equipment. Instead of crystallization dishes, capped quartz tubes (30 mL) were used as reactors. Sterilized tubes were filled with 25 mL 10 mM pH 8 sodium phosphate buffer, 1uM pCBA, and 10^{4}-10^{5} CFU mL^{-1} *B. subtilis* spores. The addition of FAC marked the start of an experiment at time, t=0.

An aluminum sleeve was slipped on each quartz tube to cover reactors in "dark" conditions or to maintain dark conditions prior to the start of an experiment (Figure 2.4). For irradiated reactors, the aluminum sleeve was also used to create dark conditions following the desired irradiation time. Dark and irradiated tubes were placed in a stand at an angle of 60 degrees approximately perpendicular to the path of the sunlight. The tubes were agitated prior to each sampling time but not continuously stirred. In order to avoid obstruction of the light path, a water bath was not used

21

for temperature regulation. Instead, the temperature of control reactors experiencing identical conditions to dark and irradiated reactors was measured throughout the experiment.

Figure 2.4: Outdoor quartz tube reactor set-up showing wrapped (left) and un-wrapped (right) tubes angled at approximately 60 degrees toward the sun.

Spectral irradiance data was collected as described above at the beginning, middle, and end of the experiment to evaluate any variations in solar irradiance throughout the experiment. Actinometric measurements were taken as described above to estimate system fluence.

2.6 Analytical Methods

2.6.1 FAC Measurement and Ct Estimates

FAC was measured by N-N-diethyl-p- phenylenediamine (DPD) spectrophotometric analysis (*60*). This method has a lower detection limit of 2.82 μM FAC concentration. One-mL samples were diluted 3-fold into 300-μL DPD indicator and phosphate buffer solution (pH 6.2) in a 1-cm disposable cuvette. A Hach DR/4000U UV-Vis Spectrophotometer measured DPD-containing solutions at 515 nm. If the calibration curves of FAC standards did not possess an R-squared > 99%, new FAC stocks were prepared and the process was repeated.

Chlorine decay during photolysis was modeled by the following first-order exponential equation:

$$C(t) = C(0)\, e^{(-kt)} \tag{10}$$

Chlorine half-lives during photolysis were determined by solving the above as follows:

22

$$t_{1/2} = \ln(2)/k \tag{11}$$

FAC Ct values during irradiation were calculated by integrating Equation 10 over a given time period. In the absence of irradiation, chlorine concentration was integrated over time by means of trapezoidal Riemann sums to determine Ct values.

2.6.2 Spore Inactivation

Post-lag phase spore inactivation was modeled according the Chick-Watson law of inactivation and was based on the assumption of first order kinetics and spore homogeneity. For regulatory and discussion purposes, spore inactivation was modeled using $\log_{10}(N/N_0)$, which requires a simple 2.303-factor conversion from the following natural log scale equation:

$$\ln(N/N_0) = -kCt \tag{12}$$

where N_0 is the initial spore concentration, N is the spore concentration remaining at time (t), k is the pseudo-first order rate-constant of inactivation, and Ct is the FAC integrated exposure determined as described above. In practice, the level of spore inactivation refers to a value of $-\log(N/N_0)$.

In order to account for the existence of a shoulder or lag phase in spore inactivation curves prior to inactivation according to first-order kinetics, the above relationship can be modified to yield the delayed Chick-Watson model as in Rennecker et al. (1999) (65):

$$\frac{N}{N_0} = \begin{cases} 1 & \text{if } CT \leq CT_{\text{lag}} = \frac{1}{k}\ln\left(\frac{N_1}{N_0}\right) \\ \frac{N_1}{N_0}\exp(-kCT) = \exp\left(-k\{CT - CT_{\text{lag}}\}\right) & \text{if } CT > CT_{\text{lag}} = \frac{1}{k}\ln\left(\frac{N_1}{N_0}\right) \end{cases} \tag{13}$$

In the above, N_1/N_0 refers to the intercept with the y-axis when extrapolating the pseudo-first

order line established by the post-lag rate constant, *k*.

2.6.3 pCBA Measurement and HO$^{\bullet}$ Ct Estimates

The loss of pCBA in the system was measured to determine HO$^{\bullet}$ concentration. pCBA reacts quickly with HO$^{\bullet}$ ($k_{HO\bullet,pCBA}$=5 x 10^9 M^{-1} s^{-1}) but not with FAC and is therefore a useful tool to quantify HO$^{\bullet}$ exposure in the presence of FAC, similar to prior applications addressing HO$^{\bullet}$ measurement in the presence of O$_3$ (*66*). Futhermore, light screening or HO$^{\bullet}$ scavenging by the system (*i.e.*, by phosphate buffer or *B. subtilis* spores) is implicitly accounted for when monitoring the degradation of pCBA.

pCBA was quantified by high-performance liquid chromatography with UV detection (HPLC-UV) on an UltiMate 3000 HPLC, using a Supelco Ascentis C18 column (150 $\times$ 2.1 mm, 3 μm). The HPLC method was isocratic with acetonitrile and 50 mM H$_3$PO$_4$ as mobile phases and absorbance detection at 205 nm (10 μL injection volume, 0.2 mL/min flow, and 4.9 minute retention time)

HO$^{\bullet}$ exposure in (mg-min) L^{-1} were calculated according to the following (*40, 66, 67*):

$$\int_0^t [\text{HO}^{\bullet}] dt = \frac{k'_{HO\bullet,pCBA,T}t - k'_{HO\bullet,pCBA,d}t}{k_{HO\bullet,pCBA}} = \frac{-\ln\left(\frac{[\text{pCBA}]}{[\text{pCBA}]_0}\right) - k'_{HO\bullet,pCBA,d}t}{k_{HO\bullet,pCBA}} \sim (Ct)_{HO\bullet}$$

(14)

where *k'*$_{HO\bullet,pCBA,T}$ in s^{-1} is the total observed pseudo-first order rate constant for pCBA loss, *k'*$_{HO\bullet,pCBA,d}$ in s^{-1} the pseudo-first order rate constant for pCBA loss by direct photolysis (in absence of FAC), and *k'*$_{HO\bullet,pCBA}$ (=5 x 10^9 M^{-1}s^{-1}) is the second-order rate constant for reaction of HO$^{\bullet}$ with pCBA (*44*).

2.6.4 PNA Quantification

PNA degradation was measured by HPLC using an isocratic method with acetonitrile and 10 mM H_3PO_4, and the same Supelco Ascentis C18 column (150×2.1 mm, 3 µm) as for pCBA quantification ($\lambda = 300$ nm, 20 µL injection volume, 0.2 mL/min flow, and 7.48 minute retention time).

2.6.5 Natural Water Characterization

Concentrations of inorganic carbon (alkalinity as HCO_3^-/CO_3^{2-} in mg L^{-1}) and non-purgeable organic carbon (Total Organic Carbon (TOC) in mg L^{-1}) in natural water samples were measured using a Shimandzu TOC-V_{CSH} analyzer. The spectral absorbance of natural organic matter (NOM) present in natural waters was determined spectrophotometrically by scanning between 200-400 nm. The spectral absorbance curves were used to determine the Specific UV Absorbance value at λ=254nm (SUVA$_{254}$ in L mg^{-1} m^{-1}) calculated by dividing the absorbance by TOC. The SUVA value is proportional to percent aromaticity of carbon and is often also related to hydrophobicity of the NOM present (68).

3. RESULTS AND DISCUSSION

3.1 Light Spectra and Actinometry

Solar light reaching the earth's surface includes ultraviolet (UVA/UVB), visible, and infrared wavelengths spanning 280 to 3,200 nm. The Newport solar simulator, equipped with a Dichroic Filter (DF) and Atmospheric Attenuation Filter (AAF), emits light beyond 300 nm. Due to the absorbance spectra of FAC, UVA and UVB radiation is most relevant. Figure 3.1 shows a comparison of the UVA/UVB spectral irradiance from the Newport solar simulator used during indoor bench-scale experiments and the incident irradiance from natural sunlight during outdoor experiments. Although the irradiation intensities are greater for the solar simulator by a factor of two to four, the overall spectral shapes are similar.
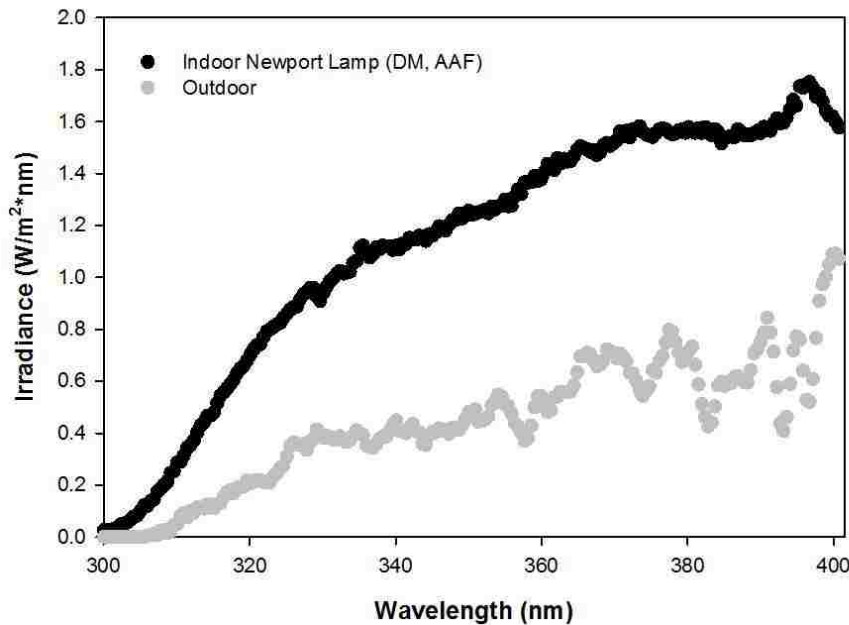

Fig 3.1: Spectral irradiance in the UVA/UVB range from the Newport Solar Simulator (with DM and AAF) and natural sunlight on the roof of More Hall, CEE, Seattle, WA at 12:00PM on May 14, 2012. Radiometric measurements taken using an Ocean Optics USB2000+ XR spectroradiometer.

26

www.manaraa.com

While absolute irradiance is useful for understanding the intensities of light emitted, it is also used to determine the flux of photons absorbed by the system (the dose of irradiation a system actually receives). Fluence, or the flux of photons integrated over time, can be measured using a chemical actinometer. The PNA/Pyr chemical actinometer was chosen since PNA loss can be monitored with HPLC-UV and the quantum yield is known (fixed value of 0.00468 M of PNA degraded per einstein in a 10 mM pyridine solution between 316 and 366 nm (63). Figure 3.2 depicts a representative plot of PNA degradation over time when exposed to radiation from the Newport solar simulator.
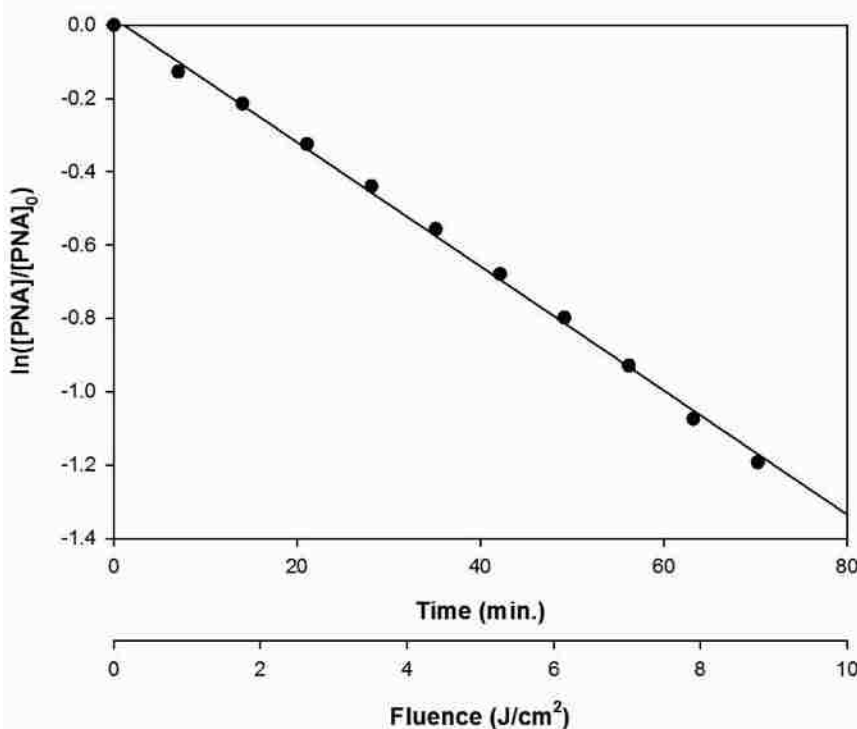
Fig 3.2: PNA loss versus time and fluence. Conditions: [PNA] = 50 µM, [Pyridine] = 10 mM, Temperature = 25 °C, and simulated sunlight with DM and AAF. Regression fit: y=-0.017x + 0.0188, R^2=0.998.

An actinometer approximates fluence in a matched system of interest most accurately if the system of interest and the actinometer have similar spectral absorbance curves. Similarities are often assessed on the basis of peak absorbance and the overall shape of the absorbance curve. The PNA/Pyr actinometer was selected as a close approximation based on absorbance curve shape between 300-400 nm. However, the peak absorbance of our system (with FAC as the predominant UV-absorbing component) is pH-dependent and slightly lower than PNA's peak

27

absorbance at each pH studied. The peak absorbance of the pH 8 FAC system was approximately 292, representative of an OCl- dominated solution, whereas the peak absorbance of the PNA/Pyr system is closer to 317 nm.

3.2 FAC Photolysis Rates

Since the rates of FAC photolysis and subsequent $HO^{\bullet}$ generation vary depending on spectral irradiance, trends in the rates were assessed using the Newport solar simulator across six different pH and temperature conditions: pH 6, 7, and 8 and 10 and 25 °C. Figure 3.3 shows how FAC photolysis rates vary with pH due to FAC speciation and temperature, at both 10 and 25 °C. As expected based on differences in HOCl and OCl$^-$ absorbance, FAC photolysis rates increase with pH as OCl$^-$ becomes the dominant species at both temperatures. Similarly, FAC photolysis rates increase with temperature due to heightened chemical reactivity and energy in the system.
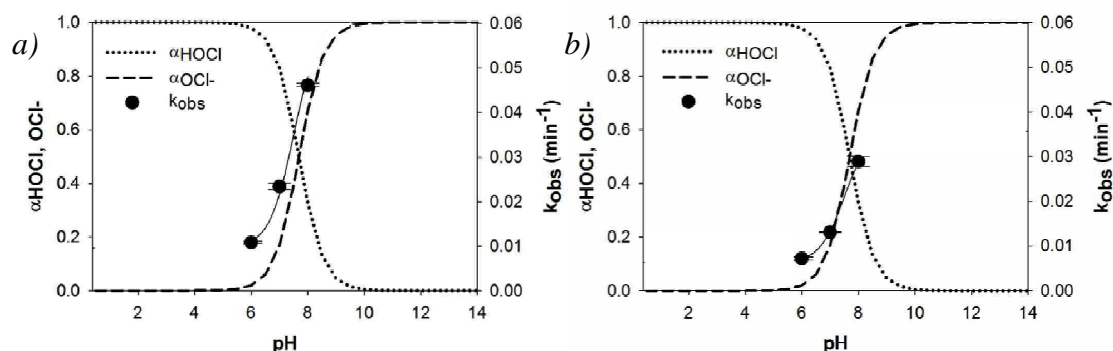

Figure 3.3: FAC photolysis rate constants plotted with FAC speciation at a) 25 °C and b) 10 °C.

At 25°C, average FAC half-lives were 15 minutes for pH 8, 30 minutes for pH 7, and 64 minutes for pH 6. At 10 °C, average FAC half-lives were 24 minutes for pH 8, and 52 and 96 minutes for pH 7 and 6, respectively.

3.3 Spore Inactivation—Phosphate-buffered Solutions, Simulated Sunlight

3.3.1 Basic Trends: pH 8, 25 and 10 °C

Initial experiments conducted using phosphate-buffered solutions at pH 8 and 25°C showed several key trends, when values of $\log_{10}$ inactivation were plotted versus FAC Ct. (Figure 3.4). Overall, the delayed Chick-Watson model accurately represented spore inactivation. With FAC but no irradiation, spore inactivation was slow with a lag phase followed by pseudo-first order kinetics. However, a reduction in lag phase and significant enhancement in inactivation was observed for continuously irradiated solutions containing initial FAC concentrations of 3 mg L^{-1} compared to dark solutions containing the same initial FAC concentration. The enhancement in inactivation of the continuously irradiated reactors with FAC can be attributed to HO$^\bullet$ exposure. This is confirmed by the shift in the inactivation curve of continuously irradiated reactors spiked with 50 mM t-BuOH (as a HO$^\bullet$ scavenger) to match that of dark FAC reactors with no HO$^\bullet$ exposure. Finally, there was no spore inactivation when solutions were irradiated in the absence of FAC over the entire length of the experiment (Figure 3.4b). This confirms the non-germicidal effect of the solar simulator's UVA and UVB radiation on *B. subtilis* spore viability and once again highlights the role of HO$^\bullet$ in enhancing inactivation.
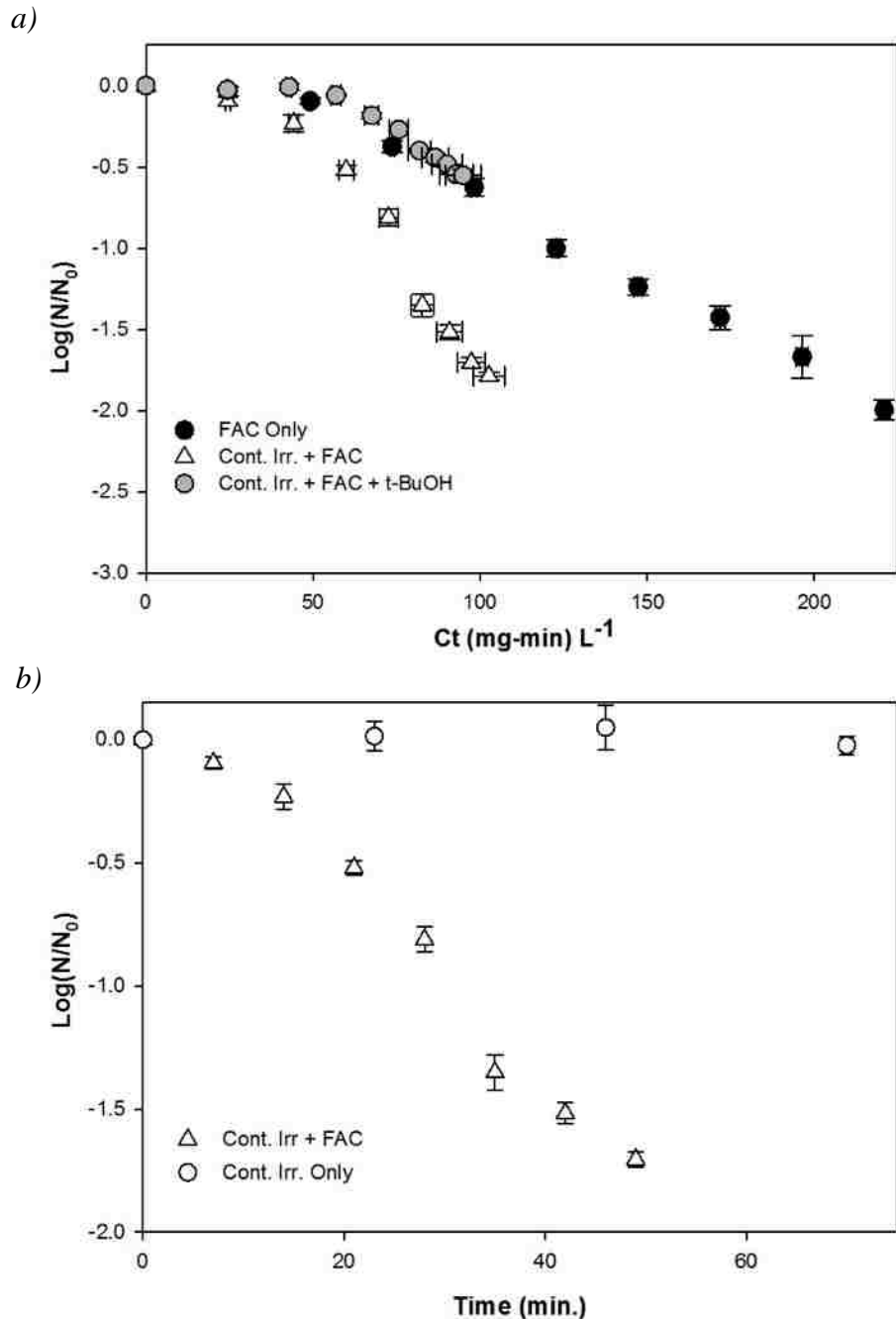
Figure 3.4: a) Spore inactivation versus Ct value with FAC but with and without irradiation and 50 mM t-BuOH as a HO• scavenger; b) Spore inactivation with irradiation but with and without FAC. Conditions: pH 8, Temperature = 25 °C, $[FAC]_0$ = 3.5 mg L^{-1}, and simulated sunlight. "Cont. Irr" refers to "Continuous Irradiation."

Despite the clear benefits of continuous irradiation with FAC on spore inactivation due to the production of HO•, continuously irradiating would be more time- and energy-intensive than irradiating for only a brief period of time. Therefore, experiments were conducted to evaluate the

effects of varying irradiation time (and therefore HO• exposure) on spore inactivation. The goal was to simultaneously maximize inactivation while minimizing irradiation time in order to optimize the process. Figure 3.5 shows that there was little added benefit to irradiation beyond a certain threshold at pH 8, 25 °C. In this set of experiments, there was approximately the same level of inactivation for a given Ct value when irradiating for 15, 30, or 70 minutes. These results indicate a reduction in lag phase and similar inactivation rates (slope) beyond 15 minutes of irradiation.
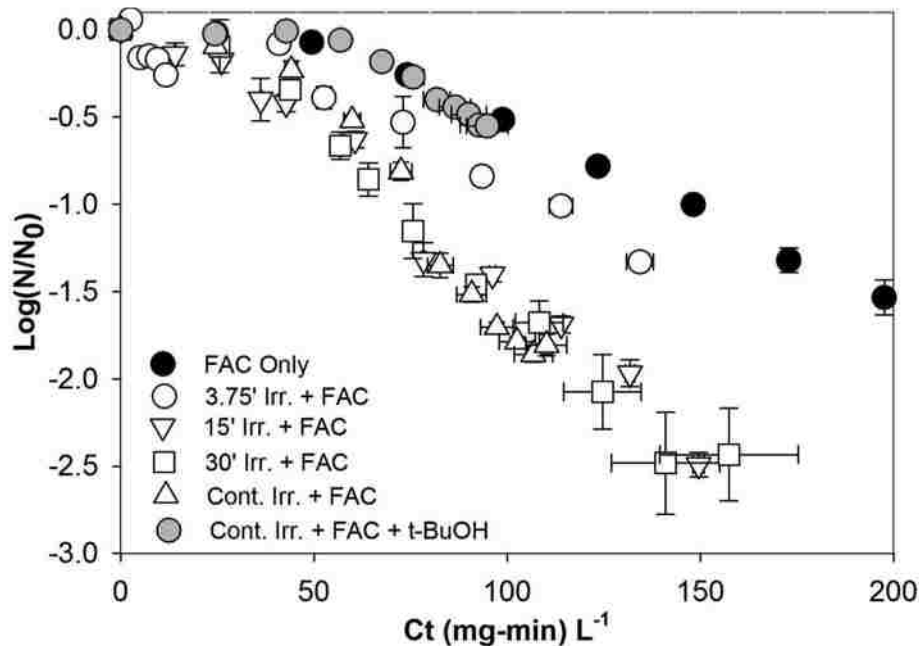
Figure 3.5: Spore inactivation versus Ct with FAC and variable irradiation time (with the exception of the continuously irradiated reactors, maximum irradiation to a Ct of 45 (mg-min) L^{-1}); Conditions: pH 8, Temperature = 25 °, [FAC]$_0$ = 3.5 mg L^{-1}, and simulated sunlight.

At pH 8, 10 °C, spore inactivation in dark FAC-only conditions, FAC with brief irradiation, and FAC with continuous irradiation were 2-3 times slower than at 25 °C, but showed similar overall trends. As expected, brief and continuous irradiation demonstrated shorter lag phases compared to dark conditions, but the inactivation rate increased more dramatically during continuous irradiation (Figure 3.6). It is important to note that the faster the rate and more vertical the inactivation curve, the greater the effect will be when targeting higher levels of inactivation (*i.e.,* three or four log$_{10}$-units of inactivation). At higher Ct values, the separation of the inactivation curves corresponding to brief and continuous irradiation would likely be magnified. However,

since the data only extends to 2 $\log_{10}$-units of inactivation, any predictions at higher Ct values would be speculative.
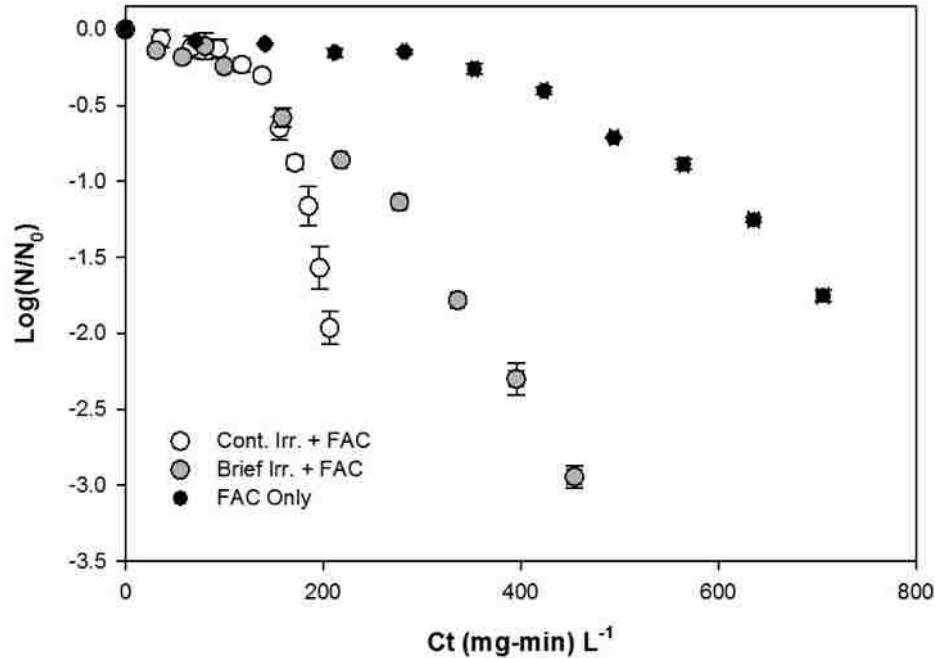
Figure 3.6: Spore inactivation versus Ct with FAC for continuous, brief, and no irradiation (brief irradiation of 22 minutes or a Ct of ~100 (mg-min) L^{-1}); Conditions: pH 8, Temperature = 10 °, $[FAC]_0$ = 3.5-8 mg/L, and simulated sunlight.

The period of brief irradiation lasted approximately 22 minutes or a Ct of ~100 (mg-min) L^{-1}, photolyzing nearly 3 mg L^{-1} FAC in order to match the starting FAC concentration of the dark reactors (Figure 3.7a). Compared to brief irradiation, continuous irradiation resulted in the photolysis of 6 mg L^{-1}, twice as much FAC. During irradiation, pCBA degradation was monitored in order to estimate HO$^\bullet$ exposure according to Equation 14 (Figure 3.7a). As seen below (Figure 3.7b), the HO$^\bullet$ exposure during continuous irradiation exceeded that of the briefly irradiated reactors by almost two-fold, consistent with the degree of FAC photolysis (Figure 3.7a). During photolysis, HO$^\bullet$ exposure increased linearly with FAC exposure. As expected, when the briefly irradiated reactors were removed from the solar simulator (at an FAC Ct of 100 (mg-min) L^{-1}), HO$^\bullet$ exposure leveled off and there was no additional HO$^\bullet$ generated during the remainder of the experiment.

32
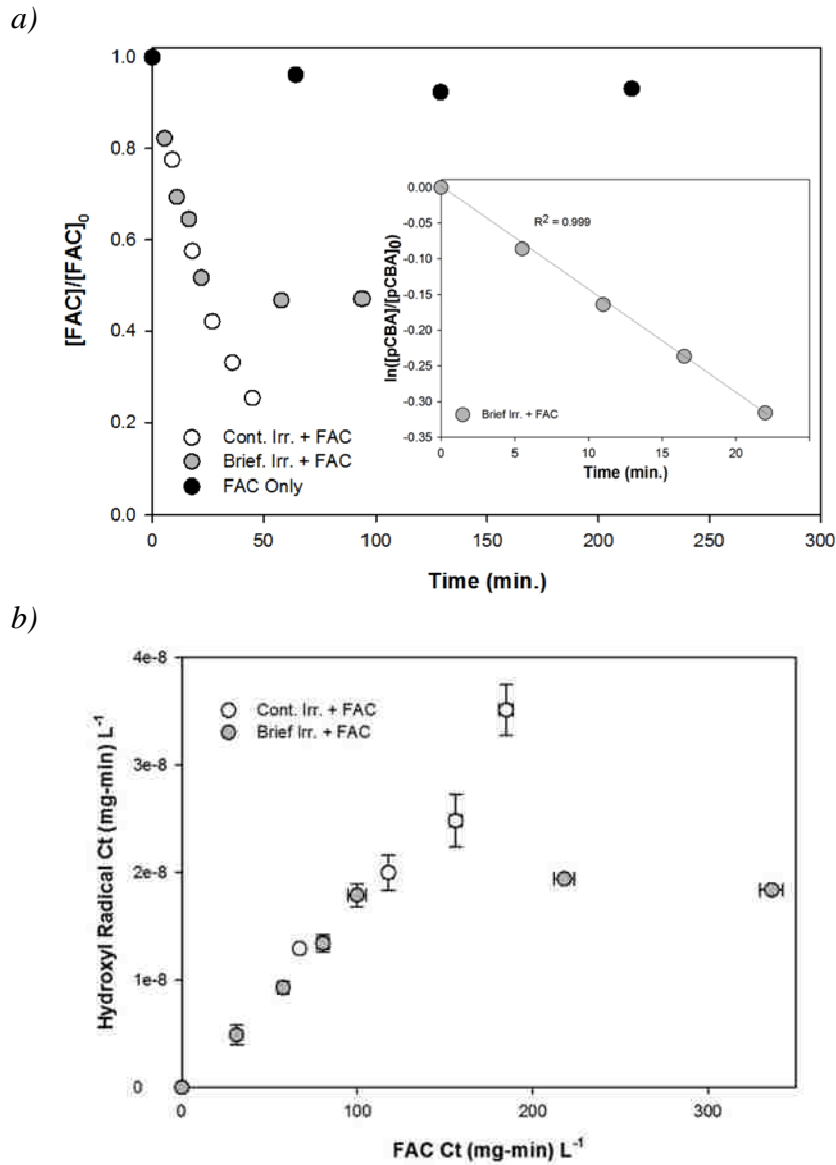
Figure 3.7: a) FAC decay versus time for continuous, brief, and no irradiation; b) pCBA loss over time for the briefly irradiated set; and c) HO⁰ exposure versus FAC exposure as Cts (mg-min) l⁻¹. Conditions: continuous irradiation [FAC]₀ ~ 8 mg L⁻¹, brief irradiation [FAC]₀ ~ 6 mg L⁻¹, no irradiation [FAC]₀ ~ 3 mg L⁻¹; pH=8 and temperature=10 °C; simulated sunlight.

3.3.2 FAC Concentration Variation

Normalizing for Ct value should allow for universal comparisons regardless of initial FAC concentrations (i.e., $[FAC]_0$=10 mg L⁻¹ for t=1 minute should be identical to $[FAC]_0$ =1 mg L⁻¹ for t=10 minutes). The hypothesis that the degree of spore inactivation achieved is independent of FAC concentration when normalizing for Ct was tested by varying $[FAC]_0$ between 1 and 8

mg L^{-1}. A series of triplicate experiments was conducted at pH 8 and 25 °C, with differing [FAC]$_0$ but the same amount of FAC photolysis (3 mg L^{-1} FAC). Each set of briefly irradiated reactors ([FAC]$_0$ =4, 6, or 8 mg L^{-1}) was paired with a set of dark reactors with [FAC]$_0$ selected to match the value remaining in briefly irradiated reactors after irradiation ([FAC]$_0$ =1, 3, or 5 mg L^{-1}, respectively). Despite differing FAC concentrations, the trends in spore inactivation for dark and brief irradiation were consistent and essentially independent of [FAC]$_0$ (Figure 3.8).
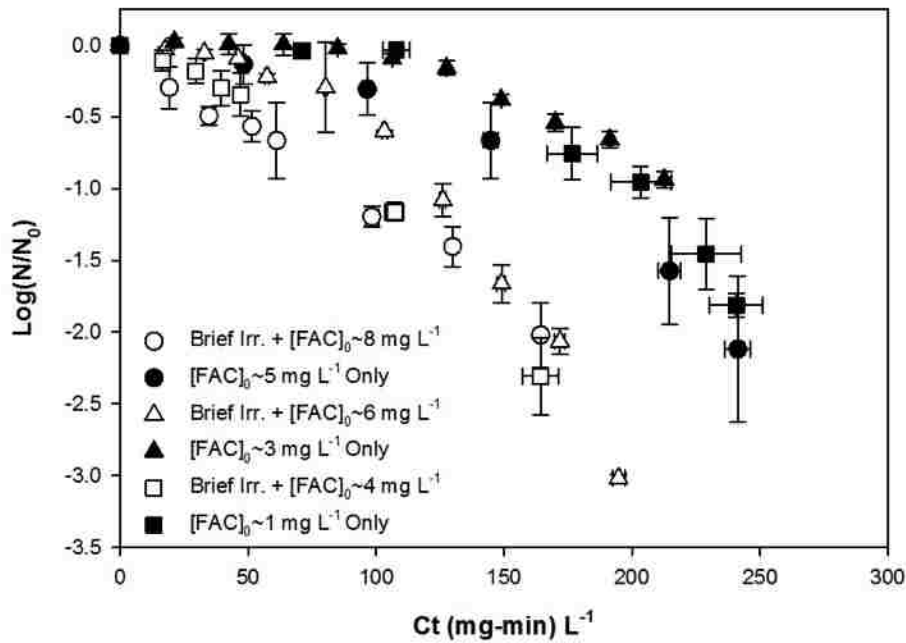
Figure 3.8: Spore inactivation versus Ct for brief or no irradiation at variable [FAC]$_0$. Conditions: Irradiated [FAC]$_0$,=4, 6, or 8 mg L^{-1}; pH=8 and temperature = 25 °C; simulated sunlight.

3.3.3 Overview of Subsequent Experiments

Given the above trends in continuous, brief, and no irradiation and a range of [FAC]$_0$ at pH 8, subsequent experiments compared brief irradiation versus no irradiation at variable pH and temperature. Most experiments were conducted using simulated sunlight from the Newport Lamp with the exception of one experiment under outdoor, natural sunlight conditions. The target pre-irradiation [FAC]$_0$ ranged from 3-6.5 mg L^{-1} and brief irradiation periods were calculated on the basis of HO$^•$ yields and FAC photolysis rates to generate approximately the

same concentration of HO$^{\bullet}$ and photolyze the same amount of FAC at each pH (*i.e.,* 1, 2, and 3 mg L^{-1} at pH 6, 7, and 8, respectively). This allowed for similar pH-specific HO$^{\bullet}$ exposures. Twelve experimental conditions were selected to evaluate the effects of pH and temperature variation: no irradiation and brief irradiation from simulated sunlight at pH 6, 7, and 8, and at 10 and 25 °C. The effect of NOM present in natural waters at 10 °C and phosphate-buffered solutions in natural sunlight at ambient temperature were also assessed.

Inactivation can be described by inactivation rate (the pseudo-first order rate constant, *k,* in L (mg-min)$^{-1}$), lag phase duration (in Ct units), and Ct value at a certain level of inactivation (in (mg-min) L^{-1}). Enhanced inactivation will be referred to on the basis of comparisons between these three parameters. The Ct$_{99}$ value refers to the Ct required to achieve 99% reduction in spore concentration or 2 log$_{10}$-units of inactivation. The Ct$_{99}$ value is highly informative since it implicitly takes lag phase length and inactivation rate into account. The Environmental Protection Agency (EPA) and other regulatory bodies commonly refer to Ct values required to achieve 2, 3, or 4 log$_{10}$-units of inactivation and thus reporting the observed Ct$_{99}$ values can provide practical information for policy-makers. Similarly, researchers commonly report Ct values for certain levels of inactivation so Ct$_{99}$ values can also be compared to published values. The Ct$_{99}$ reduction factor is the ratio of the Ct$_{99}$ value in the dark to the Ct$_{99}$ value with irradiation. The Ct$_{99}$ reduction factor is the primary tool to compare inactivation enhancements from irradiation. Additional parameters developed to elucidate the effects of irradiation on inactivation include the lag phase reduction factor and the rate enhancement factor as well as the Ct$_{99}$ savings. The Ct$_{99}$ savings was calculated as the difference (dark – irradiated) between Ct$_{99}$ or Ct necessary to achieve 2 log$_{10}$-units of inactivation. Table 3.1 provides a summary of these values for each experimental condition tested.

Table 3.1: Summary of B. subtilis spore inactivation results from all experiments: phosphate-buffered and natural waters with conditions ranging from 10 to 33°C in artificial and natural sunlight and from pH 6-8. All values are given as ± 1SE. The inactivation rate constant, k, is in units of 10^{-2} L (mg-min)$^{-1}$; Ct values are in units of (mg-min) L^{-1}. "En. Factor" is the enhancement factor (ratio of light:dark rate constants) and "Red. Factor" refers to the reduction factor (ratio of dark:light Ct$_{99}$).

Temp. (°C)	pH	Irr. time (min)	Inactivation Rate		Lag Phase		Ct$_{99}$		
			k	En. Factor	Ct	Red. Factor	Ct$_{99}$	Red. Factor	Ct$_{99}$ Savings
33[a]	8	9	13.3 (±0.3)	2.57 (±0.20)	57.8 (±0.3)	1.90 (±0.01)	92.3 (±0.5)	2.15 (±0.02)	106.2 (±7.9)
		0	5.2 (±0.3)		109.6 (±2.1)		198.5 (±7.9)		
25	8	12	5.4 (±0.3)	2.95 (±0.33)	75.0 (±7.9)	1.35 (±0.04)	161.1 (±5.0)	2.20 (±0.03)	193.6 (±18.9)
		0	1.8 (±0.1)		101.1 (±5.1)		354.7 (±15.7)		
	7	27.5	16.2 (±1.6)	2.15 (±0.21)	39.1 (±3.8)	1.05 (±0.10)	67.5 (±0.5)	1.50 (±0.01)	34.6 (±1.0)
		0	7.5 (±0.1)		41.0 (±0.6)		102.1 (±1.1)		
	6	28	17.0 (±0.5)	1.34 (±0.06)	31.8 (±0.4)	1.01 (±0.04)	58.9 (±0.5)	1.16 (±0.01)	9.7 (±0.7)
		0	12.7 (±0.7)		32.2 (±1.2)		68.6 (±1.1)		
10	8	22	1.74 (±0.0)	1.83 (±0.02)	90.4 (±12.3)	3.5 (±0.03)	355.7 (±5.1)	2.25 (±0.00)	445.5 (±8.4)
		0	0.95 (±0.0)		316.4 (±10.0)		801.2 (±11.9)		
	7	45	3.5 (±0.3)	1.64 (±0.14)	98.0 (±2.5)	1.84 (±0.02)	229.1 (±13.9)	1.73 (±0.04)	166.9 (±16.1)
		0	2.1 (±0.1)		180.4 (±6.7)		396.1 (±8.6)		
	6	50	4.0 (±0.1)	1.17 (±0.06)	76.5 (±5.7)	1.18 (±0.10)	192.5 (±5.7)	1.18 (±0.05)	33.9 (±11.5)
		0	3.4 (±0.1)		90.5 (±3.5)		226.4 (±5.9)		
	7.36[b]	22	1.0 (±0.0)	1.12 (±0.07)	157.0 (±9.6)	3.05 (±0.02)	601.9 (±20.9)	1.63 (±0.02)	377.4 (±21.9)
		0	0.9 (±0.0)		479.5 (±9.1)		979.3 (±9.6)		
	7.34[c]	22	2.1 (±0.2)	1.47 (±0.22)	191.6 (±18.2)	1.32 (±0.08)	410.0 (±4.8)	1.40 (±0.02)	165.4 (±15.5)
		0	1.4 (±0.1)		253.5 (±3.0)		575.4 (±11.9)		

a: natural sunlight (outdoor), b: natural water sample from Marysville, c: natural water sample from Cedar.

3.3.4 pH and Temperature Effects with FAC Only

As expected, dark inactivation (FAC only) was inversely related to pH due to FAC speciation at both 25 °C and 10 °C. The Ct_{99} and lag phase duration increased and the inactivation rates decreased with increasing pH (Table 3.1). At 25 °C, the Ct_{99} at pH 8 was approximately five times greater than the Ct_{99} at pH 6, extending the Ct_{99} by 286 (mg-min) L^{-1} compared to pH 6 (Ct_{99} of 355 at pH 8 compared to 69 (mg-min) L^{-1} at pH 6). The results are comparable to the findings from other researchers reporting a four-fold variation in Ct_{99} values for *B. subtilis* spores exposed to FAC between pH 8.2 and 5.6: Ct_{99} of 400 (mg-min) L^{-1} at pH 8.2 versus 90 (mg-min) L^{-1} at pH 5.6 at 25 °C (*40*).

At 10 °C, the Ct_{99} values at pH 8 were 3.5 times greater than at pH 6. This resulted in a delay of 574 (mg-min) L^{-1} to reach two $\log_{10}$-units of inactivation (Ct_{99} at pH 8 of 801 (mg-min) L^{-1} versus 226 (mg-min) L^{-1} at pH 6). The pH-dependence of inactivation can be explained by the ratio of the more effective FAC species, HOCl, to the less potent form, OCl$^-$, at each pH. The fraction of HOCl (α_{HOCl}) at pH 6, 7, and 8 at 25 °C is approximately 0.97, 0.74 and 0.24, respectively.

The Ct_{99} values at each pH at 10 °C were more than 2-3 times greater than the corresponding Ct_{99} for each pH at 25 °C. However, it is unclear why the relative inactivation at pH 7 compared to pH 6 and 8 was faster at 25 °C than 10 °C (Figure 3.9). The slower inactivation at lower temperature can be attributed to chemical kinetics and the activation energy barrier of FAC reactions. The results are similar to the temperature dependence described by Li et al. (2001) (*69*) investigating *C. parvum* disinfection between 1 and 25 °C. They described a 2.2-fold decrease in inactivation for every 10 °C decrease in temperature. They estimated the activation energy for the reaction to be 52 kJ mol^{-1} using rates of inactivation at a target and reference temperature. Temperature effects can be modeled using the van't Hoff-Arrhenius equation given inactivation rate data at several temperatures (*28, 69*).
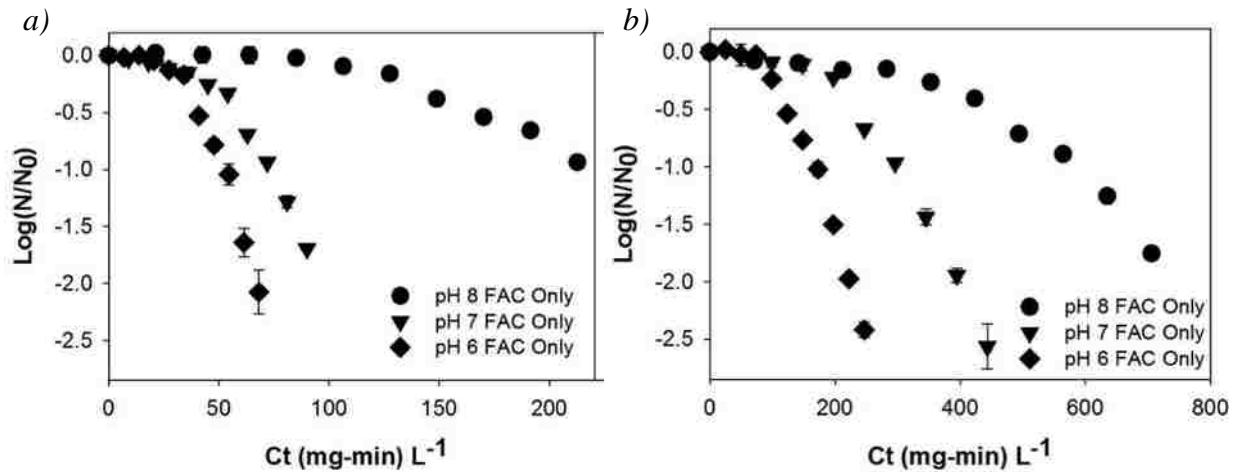
Figure 3.9: Spore inactivation versus Ct in the absence of irradiation with $[FAC]_0 \sim 1, 2, 3$ mg L^{-1} at pH 6, 7, or 8, respectively; a) at 25 °C; b) at 10 °C, simulated sunlight.

3.3.5 pH and Temperature Effects with Irradiation and FAC

At both 10 and 25 °C, pH was the most important determinant of the enhancement effect from irradiation. The impact of irradiation on inactivation was positively associated with pH. For example, the values of the rate enhancement factor, lag phase reduction factor, and Ct_{99} reduction factor value all increased from pH 6 to pH 8 (Table 3.1). This may be explained by the nature of HO$^{\bullet}$. In comparison to FAC, HO$^{\bullet}$ effectiveness as a disinfectant is less pH-dependent since the latter is not prone to speciation. Therefore, at higher pH, when FAC reactions are slow but HO$^{\bullet}$ reactions do not change, the enhancing effect is more evident.

Temperature exerted a less significant effect on enhancement than pH. At 25 °C, the differences between irradiation versus no irradiation are less apparent than they are at 10 °C since the rates of all reactions are faster at higher temperatures (Figure 3.10a). At 10 °C there is greater separation between curves due to slower rates of FAC-only reactions so the enhancing effect can be seen clearly at pH 8 and 7, and to a lesser extent, at pH 6 (Figure 3.10b).

a)

b)
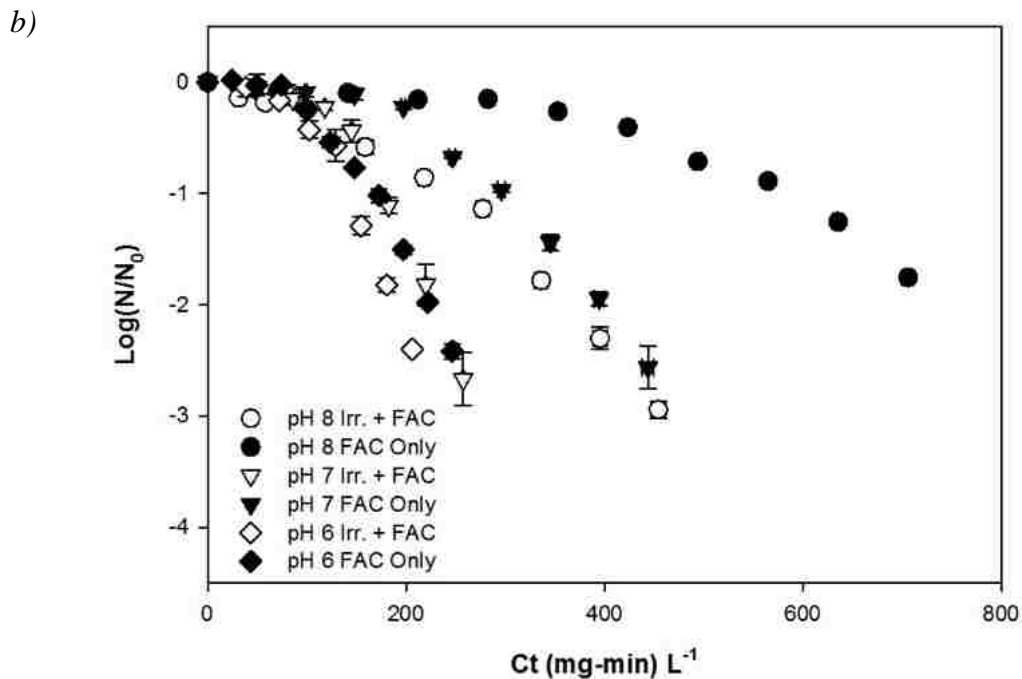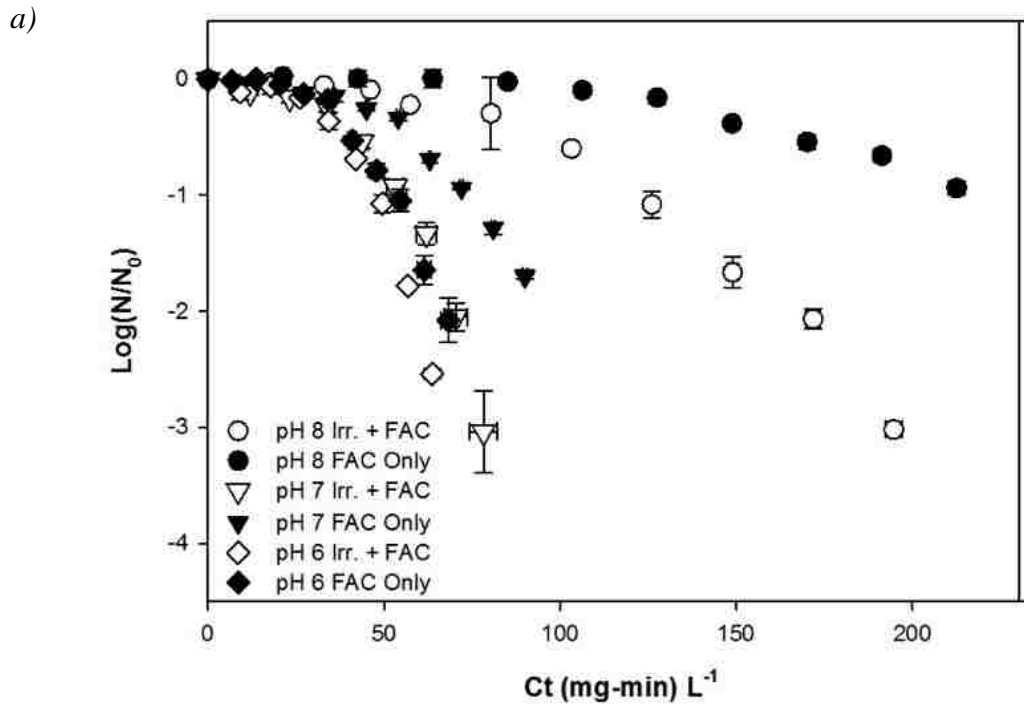
Figure 3.10: Spore inactivation versus Ct with and without irradiation with $[FAC]_0$ between 1 and 6 mg L^{-1} at pH 6, 7, or 8 at a)25 °C and b) 10 °C, simulated sunlight. Since the length of chlorine's half-life increases with decreasing pH and spore inactivation rate also increases with decreasing pH, it was impossible to have a light-then-dark approach at pH 6 and 7 at 25 °C so these were continuously irradiated. At pH 8, half the FAC or 3 mg L^{-1} was photolyzed over a period of 12 minutes followed by 56 minutes with FAC only and no irradiation.

39

At both temperatures, the enhancing effect of irradiation resulted in faster inactivation rates, shorter lag phases, and lower Ct_{99} values than would be expected with FAC alone. When comparing the irradiated versus dark conditions, temperature exerted opposite effects on the inactivation rate and the length of the lag phase at 25 and 10 °C. At 25 °C, the rate enhancement factors were 1-2 times higher than at 10 °C. Meanwhile, at 25 °C the lag phase reduction factors were 1-2 times lower compared to 10 °C. These trends appeared to counterbalance each other by resulting in Ct_{99} reduction factors that differed by less than 10% for a given pH at 10 and 25 °C (i.e., Ct_{99} reduction factors at pH 8 of 2.2 and 2.25 at 25 and 10 °C, respectively). As demonstrated by Figure 3.11, the relationship between Ct_{99} reduction factors and pH is linear and apparently independent of temperature. It should be noted here that since only two temperatures were compared, it is not possible to make extensive conclusions about effects of temperatures less than 10 and greater than 25 °C. The temperature independence of the Ct_{99} reduction factors may be explained by similarities in activation energies of FAC and $HO^{\bullet}$. Although activation energies for $HO^{\bullet}$ reactions with spores have not been derived, activation energies of FAC with *B. subtilis* spores of 84 kJ mol^{-1} have been reported (*70*). If activation energies of $HO^{\bullet}$ with spores were similar, the effect of changing temperature would result in comparable changes in reactivity of both FAC and $HO^{\bullet}$, making the enhancement effect of irradiation temperature independent.
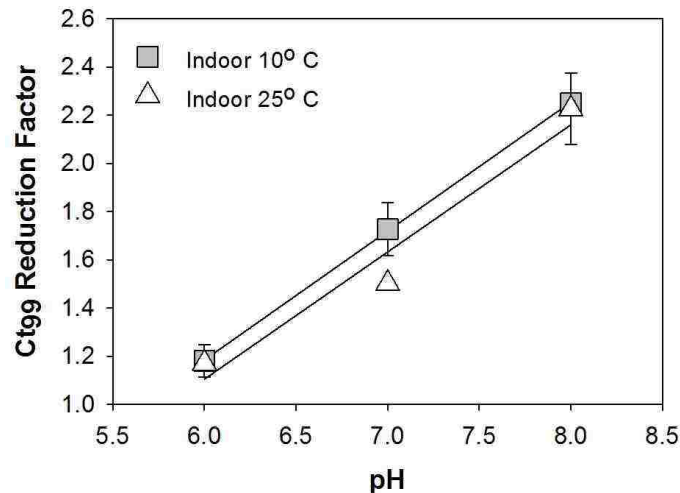

Figure 3.11: Ct_{99} Reduction Factors (ratio of dark Ct_{99} to irradiated Ct_{99}) versus pH for both 10 and 25 °C datasets, simulated sunlight. For 10 °C, regression equation of y=0.54x-2.05, R^2=0.999. For 25 °C, y=0.52x-2.0, R^2=0.965.

Furthermore, despite similar Ct_{99} reduction factors at each temperature for a given pH, it is important to note that the enhancement in inactivation at 10 °C would be more beneficial in terms of overall Ct and time savings. The Ct_{99} savings at pH 8, 10 °C, for example, is 445 (mg-min) L^{-1} versus only 193 at 25 °C. Similarly, the t_{99} savings at all pH conditions was two to three-fold greater at 10 °C compared to 25 °C. At pH 8, 10 °C, the t_{99} for dark conditions was over 240 minutes but only 100 minutes with irradiation. The significant spore inactivation enhancement *and* time-saving benefit of FAC with irradiation at 10 °C is promising and highly relevant to drinking water treatment in temperate climates.

3.4 Spore Inactivation—Natural Waters, Simulated Sunlight

3.4.1 Natural Water Characteristics

Water samples from the Marysville and Cedar water treatment facilities were taken before FAC treatment would be administered during normal operations in order to test the potential enhancement of spore inactivation by $HO^{\bullet}$ exposure in representative drinking waters containing NOM. Since the temperatures of the waters were between 6 and 8 °C at the treatment plants, the experiments were conducted at 10 °C to approximate real-world conditions and to facilitate comparisons with phosphate-buffered solutions.

Table 3.2 shows the characteristics of the Marysville and Cedar waters in terms of pH (7.36 and 7.34) and $SUVA_{254}$ values (2.25 and 2.28 L mg^{-1} m^{-1}). Despite similar $SUVA_{254}$ values, the organic carbon content was less and the absorbance at 254 nm was greater for Marysville compared to Cedar water. The waters also differed in terms of total carbonate alkalinity. The total alkalinity, predominantly as HCO_3^-/CO_3^{2-} at circumneutral pH, was more than four times higher in the Marysville sample than in the Cedar water. Overall, however, TOC and alkalinity were relatively low for each sample, and considered to be representative of drinking waters in the region.

Table 3.2: Water characteristics of natural water samples from the Landsburg Diversion at the Cedar River Water Treatment Plant and the Marysville Water Treatment Plant near Seattle, WA.

Water Source	pH	TOC (mg L^{-1})	Alk. (mg L^{-1})	$SUVA_{254}$ (L mg^{-1}-m^{-1})
Marysville WTP	7.4	0.6	9.8	2.3
Cedar WTP	7.4	1.2	2.1	2.3

3.4.2 Inactivation Trends

As expected, both waters exhibited slower inactivation rates, longer lag phases, and higher Ct_{99} values than would be predicted based on pH alone compared to the phosphate-buffered solutions (Figure 3.12, Table 3.1). However, despite lower TOC, and relatively similar NOM characteristics of the two waters, the overall spore inactivation (with and without irradiation) was considerably slower for the Marysville than the Cedar water. For example, the Ct_{99} of Marysville water in dark conditions (979 (mg-min) L^{-1}) was almost twice that of Cedar water (575.4 (mg-min) L^{-1}).

Even though spore inactivation in dark conditions was slower, there was still substantial enhancement in inactivation due to irradiation in each water. In fact, the enhancement effect of brief irradiation was greater for Marysville water than Cedar water in terms of lag phase reduction (3.05 versus 1.32 reduction) and Ct_{99} reduction factors (1.63 versus 1.4) (Table 3.1). Additionally, although the steady state $HO^{\bullet}$ exposures were similar, Marysville $HO^{\bullet}$ exposure was slightly less than Cedar (2.4 x 10^{-8} compared to 2.9 x 10^{-8} (mg-min) L^{-1}). Since there was a greater enhancing effect of irradiation for Marysville despite overall slower inactivation rates compared to Cedar, this supports the hypothesis that as FAC reactions slow, the benefit of irradiation becomes more pronounced (as seen at higher pH and lower temperature).
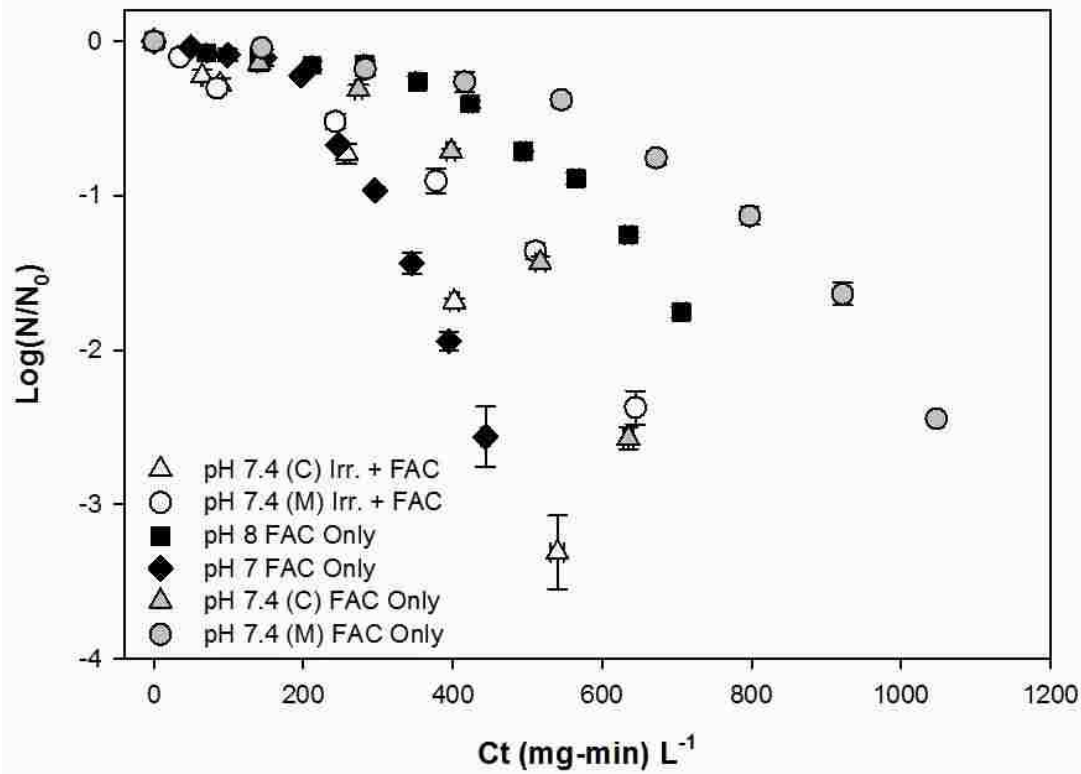
Figure 3.12: Spore inactivation versus Ct for irradiated and dark reactors from natural water samples (M=Marysville and C=Cedar) and phosphate-buffered solutions (pH 7 and 8). Simulated sunlight, Conditions: pH 7.34 (Cedar), and 7.36 (Marysville); [FAC]$_0$ =variable (2-6 mg L^{-1}); Temperature = 10 °C.

The enhancement provided by irradiation in the natural water samples was marginally lower than would be expected based on the results from the phosphate-buffered solutions. Following the linear relationship between pH and Ct$_{99}$ reduction factor in Figure 3.11, a factor of approximately 1.91 would be expected for phosphate-buffered solutions at pH 7.34-7.36 at 10 °C whereas observed values were 1.63 and 1.4. This discrepancy could be explained by a number of factors related to the presence of organic matter. In addition to the HO$^{\bullet}$ scavenging capacity of NOM (*71, 72, 73*), NOM could also block light in the irradiated photochemical system. Nowell and Hoigné (1992) (*38*) discuss the chromophoric shielding effect of some organic matter constituents that can reduce the photolysis rate up to 50% and limit light penetration even at shallow depths. With high DOC content (4.0 mg L^{-1}) they reported photolysis of FAC up to water depths of 0.5 meters, whereas with low DOC content (0.4 mg L^{-1}), they reported FAC

photolysis up to 3 meters in depth. However, the similar rates of FAC photolysis and Ct_{99} reduction effect in the natural waters and phosphate-buffered solutions suggest that light screening did not play a major role in slowing the photochemical reactions.

In contrast to the present observations, the presence of NOM has been reported to enhance disinfection efficiency under certain conditions. Rincòn et al. (2001) (74) and Mamane et al. (2005) (39) found enhanced inactivation of *E. coli* and MS2 phage during UV/H_2O_2 generation of $HO^{\bullet}$ in natural waters compared to buffered solutions. Additionally, Cho et al. (2003) (75) demonstrated enhanced inactivation of *B. subtilis* using O_3 in the presence of NOM and Barbeau et al. (2006) (76) demonstrated a similar Ct_{99} reduction factor of 2.3-7.1 with chlorine dioxide depending on NOM concentrations. This phenomenon might be explained by NOM's role as a source and/or promoter of reactive oxygen species formation (ROS, such as $HO^{\bullet}$, H_2O_2, and $O_2^{\bullet-}$), particularly in photochemical or advanced oxidation systems, which could counter-act NOM's negative role as a disinfectant scavenger. The formation of ROS could be induced by UV/H_2O_2 in addition to O_3 or chlorine dioxide in the presence of NOM.

Interactions between amongst water matrix constituents, disinfectant, and microorganism all have the capability to impact disinfection. The significantly slower inactivation of Marysville water may be explained by interactions between spores and ionic or metallic compounds in the water. Many microorganisms, including spores and viruses, are capable of forming aggregates. *B. subtilis* spore aggregates have been reported to be on average 18 times more resistant to disinfection than single spores (76), where resistance to disinfection varied significantly according to the size of the aggregate. Barbeau et al. (2006) (76) also demonstrated pH-dependent aggregation likely related to the effect of protonation of spore constituents on cell interactions (*i.e.,* larger aggregates at lower pH).

In general, wild type or indigenous spores or spores that possess an exosporium are more likely to aggregate due to greater hydrophobicity thought to facilitate spore-spore interactions (77). Since *B. subtilis* (ATCC 6633) spores lack an exosporium, it would be surprising for aggregation to be a significant concern without aggregate-facilitating constituents in the water like metal

44

cations. In addition to spore-spore interactions, metals or other compounds may associate with spores and result in an aggregating or light shielding effect.

Either spore aggregation or complexation with metallic or ionic compounds would be expected to alter the shape of the inactivation curve. Aggregation of microorganisms most often results in a tailing effect on the spore inaction curve (*76*). This may be explained by the growing size of aggregates as more particles come in contact with one another over the course of disinfection. Although the inactivation curves for Marysville and Cedar waters did not demonstrate a tailing behavior, aggregation cannot be discounted as a possible explanation for the observed resistance to disinfection.

The higher alkalinity of the Marysville water may also impact inactivation, as carbonate species could scavenge $HO^{\bullet}$. However, since the enhancing effect of irradiation was higher in the Marysville water compared to the Cedar water, it is unlikely that the carbonate species scavenged $HO^{\bullet}$ significantly. Furthermore, the steady state $HO^{\bullet}$ exposures were very similar for the two water samples (2.4×10^{-8} for Marysville versus 2.9×10^{-8} (mg-min) L^{-1} for Cedar).

As seen by the results described above and those reported by other researchers, a disinfectant's behavior in natural waters is complex, variable, and difficult to predict. Since regulatory standards are established based on disinfection data from synthetic waters, there is a critical need for a systematic evaluation of the effects of varying concentrations and types of organic and inorganic constituents in representative waters.

3.5 Spore Inactivation—Phosphate-buffered Solutions, Natural Sunlight

3.5.1 Solar Characteristics

Due to the significant enhancement of irradiation-mediated inactivation at pH 8, the effect of natural sunlight was only tested using phosphate-buffered solutions at pH 8. The solar spectrum was very similar to the standard Terrestrial Reference Spectra reported by the American Society for Testing and Materials (ASTM). However, the natural solar spectrum differed from the

45

simulated spectrum produced by the Newport lamp, as shown above in Figure 3.1. The primary differences in the natural and simulated spectra were the intensities of light, particularly in the 300-400 nm range. The peak intensities of natural sunlight were in the visible range (data not shown), near 460 nm.

The FAC half-life during natural sunlight photolysis in clear skies at mid-day (5/14/12 at noon) was 9 minutes with a solution temperature of 10 °C. Aside from the differing physical configuration of reactors, the outdoor experimental protocol was identical to simulated sunlight experiments at pH 8. Reactors with 3 mg L^{-1} FAC in the absence of sunlight were compared to reactors initially containing 6 mg L^{-1} FAC that were exposed to sunlight for 9 minutes in order to photolyze 3 mg L^{-1} FAC after which the reactors were shielded from light.

3.5.2 Inactivation Trends

Overall, the Ct_{99} values for dark and irradiated reactors were lower during the outdoor experiment than the bench-scale pH 8 25 °C experiments due to the higher temperature of both dark and irradiated reactors (33 °C) (Figure 3.13). Despite differences in spectral intensity between natural and simulated sunlight, the spore inactivation enhancement effect of irradiation matched that at 25 and 10 °C of simulated sunlight. The mean Ct_{99} reduction factor for these experiments was 2.15, compared to 2.20 and 2.25 at 25 and 10 °C (Figure 3.14). The 2.15 factor reduction in Ct_{99} due to natural sunlight irradiation resulted in a Ct_{99} that was 106 (mg-min) L^{-1} less than the Ct_{99} of the FAC-only dark conditions.
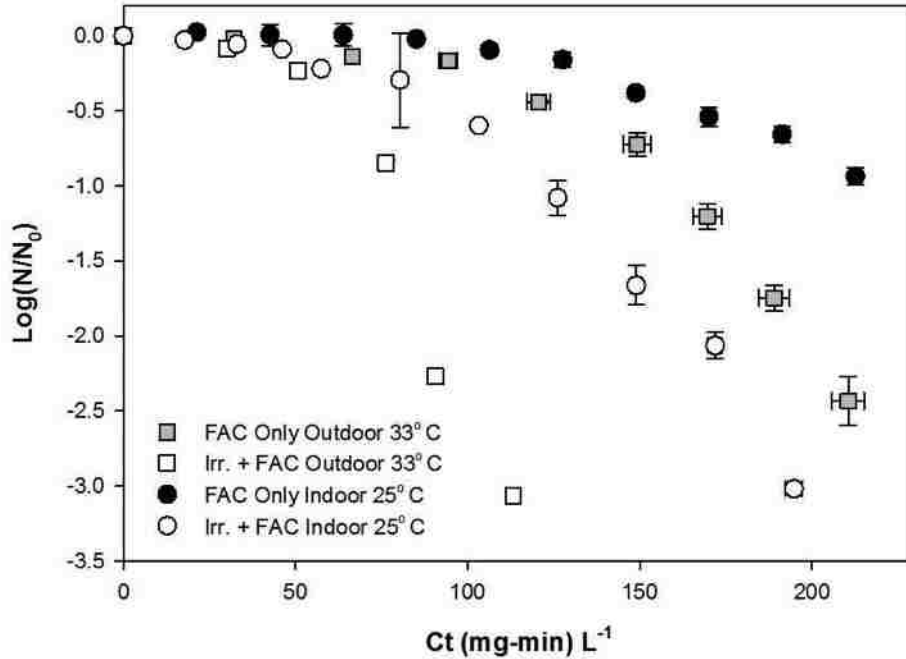
Figure 3.13: Comparison of spore inactivation versus Ct in the absence of irradiation and in simulated sunlight (25 °C) and natural sunlight (on the roof of More Hall, 5/14/2012 at noon, 33 °C). Conditions: phosphate-buffered solutions, pH 8, with dark $[FAC]_0 \sim 3$ mg L^{-1} and irradiated $[FAC]_0 \sim 6$ mg L^{-1}.
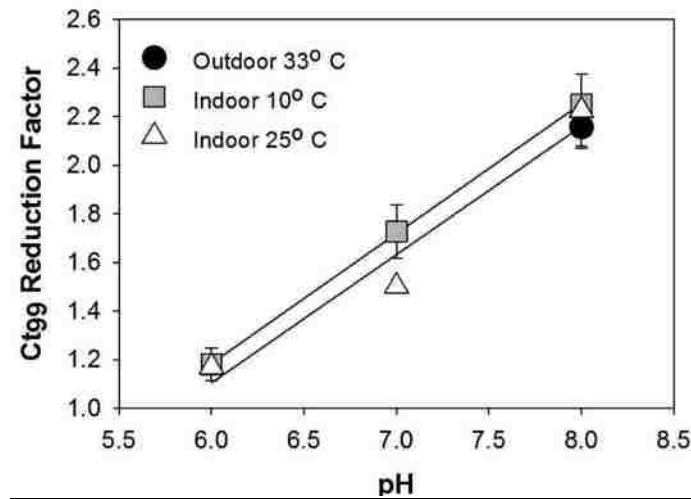
Figure 3.14: Ct_{99} Reduction Factors versus pH from simulated sunlight (at 10 and 25 °C) and natural sunlight (at 33 °C).

One possible explanation for the similar inactivation despite less intense light in the outdoor experiments may be the differences in irradiate surface areas for each type of reactor. In an outdoor environment, the light comes from all angles as it is reflected and refracted along its path. In the Newport simulator, however, the light is emitted as a semi-collimated beam where

the light comes from the source in a single beam with minimal dispersion. This additional exposure to light in the outdoor environment may compensate for the lower intensity of light. This was confirmed by similarities in fluence between the simulated and natural sunlight experiments.

3.6 Disinfection-by-product Concerns

In addition to the effects of the presence of NOM on disinfection efficiency, possible routes of disinfection-by-product formation must be addressed. Both chlorine-based and photochemical reactions have the potential to generate carcinogenic DBPs. In fact, one of the primary disadvantages of chlorine-based disinfection that motivated a shift toward the use of alternative disinfectants is the formation of organohalides such as trihalomethanes (THMs) or haloacetic acids (HAAs) (*49*).

It is possible that the photochemical system studied here using both FAC and HO$^{\bullet}$ disinfection could result in the formation of halogenated organics from FAC and additional DBPs from HO$^{\bullet}$ reactions. Several studies have indicated that O$_3$-based disinfection can result in the formation of BrO$_3^-$ or other brominated DBPs. For example, in waters with high concentrations of Br$^-$, O$_3$ or HO$^{\bullet}$ could oxidize HOBr to form BrO$_3^-$, which would not be possible from disinfection by FAC alone (*78, 79*). Furthermore, HO$^{\bullet}$ has been shown to oxidize FAC to ClO$_3^-$ (*80*) which may be further oxidized to ClO$_4^-$ (*81*). Both ClO$_3^-$ and ClO$_4^-$ are DBPs of concern.

Although photochemical enhancement of chlorination could lead to increased DBP formation, it is also possible that the present photochemical system could actually result in lower DBP levels compared to a system with FAC alone. von Gunten et al. (2001) (*82*) found a positive linear correlation between FAC Ct values and halogenated organic compound concentrations. Therefore, the observed one-to-two-fold reduction in Ct$_{99}$ values with FAC and HO$^{\bullet}$ could translate to lower DBP levels. Similarly, lower concentrations of the DBP, CHCl$_3$, were generated during FAC photolysis than with FAC alone at a range of pH levels. This could be attributed to the degradation of FAC and lack of additional CHCl$_3$ formation from FAC photoproducts (*37*). Another interesting possibility would be the elimination of DBPs by either

HO• or *in situ* photo-degradation, or both. As suggested by Watts and Linden (2007) (*45*), HO•
may be capable of removing DBPs during realistic water treatment conditions. Furthermore,
depending on the molar absorptivity of NOM present, it could be possible for UV light to
photolyze and degrade NOM itself. Additional investigations into such processes of DBP
formation and elimination should be carried out to fully understand the implications for public
health.

3.7 Possible Mechanisms of Enhanced Inactivation

FAC-only inactivation curves possessed a substantial lag phase followed by pseudo-first order
kinetics. This type of curve is typical of FAC disinfection of *B. subtilis* spores (*75*). The length of
the lag phase may be related to FAC's weak disinfection capabilities against the spore's
protective coat that may require repeated attack to achieve inactivation (*21*). The presence of a
lag phase has been explained based on a multi-hit or multi-target theory of disinfection where
microorganisms are inactivated only when disinfectant dose or exposure exceeds a certain
threshold (*83*). This threshold Ct value marks the end of the lag phase.

With HO• exposure from FAC photolysis, *both* a shorter lag phase and a faster rate of
inactivation were observed in comparison with FAC only. Cho *et al.* (2006) (*40*) reported lag
phase removal during *B. subtilis* spore inactivation by pre-treating with O_3 or ClO_2 followed by
FAC treatment. However, HO• disinfection studies of *B. subtilis* spores have produced variable
results. For example, Mamane et al. (2005) (*39*) reported no inactivation of *B. subtilis* spores by
UV/H_2O_2 ($\lambda > 292$ nm). One possible explanation may be their use of a different strain of *B.
subtilis*, which could drastically change spore response to disinfection. Cho et al. (2011) (*58*),
however, used the same *B. subtilis* strain (ATCC 6633) and noted a reduction in lag phase, but
no change in inactivation rate compared with FAC-only disinfection using UV/H_2O_2 ($\lambda =$
254nm). Certainly, some differences between *B. subtilis* (ATCC 6633) spore response to
disinfectants could be expected based on slight differences in spore preparation that would result
in different core water content, which is thought to play a role in the spore's resistance. Factors
affecting this could include the use of broth versus agar for initial vegetative cell culture as well
as temperature and length of incubation during sporulation, among others (*84*).

49

An additional factor influencing variability in response to $HO^{\bullet}$ is the method of generating $HO^{\bullet}$ and the potential synergism of combining disinfectants. Mamane et al. (2005) (*39*) generated $HO^{\bullet}$ using non-germicidal UV light ensuring that $HO^{\bullet}$ was the only disinfectant. Cho (2011) (*58*), however, used germicidal UV_{254} so both $HO^{\bullet}$ and UV light inactivated spores. In our system, $HO^{\bullet}$ was generated by FAC photolysis and thus $HO^{\bullet}$ disinfection was concurrent with FAC disinfection. Since diffusion is not likely to play a major role in disinfection of the spores by FAC or $HO^{\bullet}$ due to the protective spore coat (*39*), it can be expected that the disinfectants must first target the outer spore coat. Due to $HO^{\bullet}$'s highly and non-selective oxidative capacity, $HO^{\bullet}$ may oxidize spore coat constituents that would otherwise be FAC-recalcitrant (*58*). Figure 3.15 represents this concept visually. This initial damage could make the coat more penetrable by $HO^{\bullet}$ or FAC and generally increase the susceptibility of the spore to subsequent attack. When $HO^{\bullet}$ generation stops, FAC could continue to attack the spore for longer time periods. Similar to the coat, the spore cortex is a protective barrier with high concentrations of peptidoglycan. Cross et al. (2003) (*85*) found that intracellular generation of $HO^{\bullet}$ within spores of *Bacillus globigii* was more effective at inactivating the spores than $HO^{\bullet}$ generated externally. Therefore, due to holes or damage to the coat, the $HO^{\bullet}$ or FAC might reach the cortex earlier and have a more pronounced effect to increase the rate of inactivation. However, in other studies, adequate damage to the spore coat alone has been shown to inactivate spores by disrupting normal spore functions (*86*).
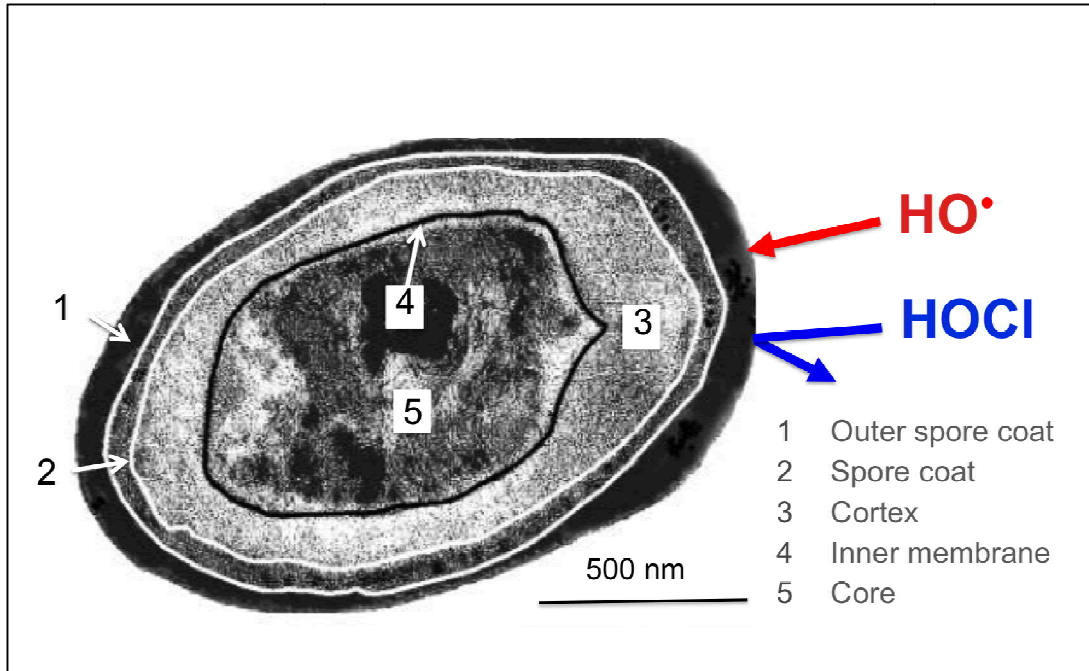
Figure 3.15: Schematic of extracellular HO• and FAC attack. (Electron micrograph image adapted from Driks et al. 1999 (86)).

4. CONCLUSIONS

4.1 Key Results

Overall, irradiation with FAC, irradiation without FAC, and dark FAC-only experiments of nine conditions were tested. These included phosphate-buffered solutions exposed to simulated sunlight at pH 6, 7, and 8 and 10 and 25 °C, and natural sunlight at pH 8 and ambient temperature, 33 °C. Two different natural water samples of pH 7.4 were tested at 10 °C in simulated sunlight. There was no spore inactivation at any pH or temperature with irradiation but without FAC at any of the conditions.

For all experimental conditions, pH was the primary determinant of spore inactivation. As anticipated, dark FAC-only experiments demonstrated a negative effect of increasing pH on spore inactivation. At pH 8, Ct_{99} values were three to five times higher than Ct_{99} values at pH 6 or 7. In both 10 and 25 °C phosphate-buffered solutions, pH was the most important determinant of the enhancement effect from irradiation with FAC. The Ct_{99} reduction factors at pH 6 were 1.16-1.18 at 10 and 25 °C versus 2.2-2.25 at pH 8.

In addition to pH, FAC-only experiments demonstrated a positive effect of increasing temperature on inactivation. Ct_{99} values at 10 °C were more than 2-3 times greater than the corresponding Ct_{99} for each pH at 25 °C. Temperature exerted a less significant effect on enhanced irradiation than pH for phosphate-buffered solutions. The enhancement effect of natural sunlight was similar to simulated sunlight at pH 8 despite different temperatures. The Ct_{99} reduction factors showed a positive linear relationship with pH that was independent of temperature (including 10, 25 and 33 °C data).

In natural waters with low NOM the enhancing effect of simulated solar irradiation was only slightly less than would be expected based on pH alone at 10 °C. However, the dark FAC-only reactions were much slower than expected. This may be attributed to spore-spore aggregations facilitated by constituents present in natural waters, such as metal cations, that were not present in phosphate-buffered solutions.

Overall, the relative benefit of enhanced inactivation from irradiation is greatest when FAC reactions are slow. For example, the most significant time and Ct savings were at higher pH, lower temperatures, and in natural waters with NOM present.

4.2 Applications

As demonstrated, this approach of photolyzing FAC to generate HO$^•$, then stopping photolysis to maintain an FAC residual could provide significant benefits at relevant pH and temperatures with natural waters and natural sunlight. The enhanced inactivation of chlorine-resistant microorganisms and the cost- and time-savings make it an attractive approach for both centralized and decentralized applications.

In a centralized setting, such as at a municipal water treatment plant, shifting from high-energy and costly germicidal UV lamps ($\lambda < 300$ nm) to lower energy solar lamps ($\lambda \sim 300$-400 nm) in combination with FAC could be less expensive and more practical. By combining solar light and FAC to achieve advanced oxidation in a single application, this could also simplify the treatment process by reducing the number of steps involved.

Furthermore, in decentralized settings such as households in developing countries, this could serve as an enhancement to traditional SODIS or chlorination methods. By combining SODIS and chlorination to generate HO$^•$, this could provide a higher level of pathogen inactivation, particularly of protozoa or helminths, than would be possible with either method alone. In addition to being more effective, this could be 2-3 times faster than chlorination and 10-20 times faster than SODIS.

4.3 Optimization and Future Work

Before implementing the enhanced FAC-sunlight process in practice, further research is required. In particular, this should include an investigation of the effectiveness of the method to

53

inactivate important chlorine-resistant human pathogens such as *Mycobacterium avium*, coxsackievirus B5 (CVB5), *C. parvum*, and *Ascaris lumbricoides*.

It is also important to more fully understand the effect of chemical constituents present in natural waters on inactivation. Specifically, future research should investigate how different types and concentrations of NOM would impact HO$^\bullet$-scavenging capacity, light screening, and FAC demand. Similarly, the impact of ionic compounds on spore aggregation merits investigation.

Additionally, a more in-depth test of different solar lamps or outdoor solar conditions would be worthwhile. It would be interesting to compare different lamps based on inactivation, but also by their cost and energy-requirements. Different lamps to consider could include Low/Medium Pressure Hg Lamps (λ = 254 nm) commonly used during UV/H$_2$O$_2$ AOPs, higher energy KrCl Excimer lamps (λ = 222nm), lower energy XeBr Excimer Lamps (λ = 282 nm), as well as UVB/UVB emitting LEDs or blacklights. This would also facilitate comparisons of energy costs for the photochemically enhanced FAC method with conventional AOP processes. By applying the FAC-sunlight process for microorganism inactivation instead of contaminant removal applications typical of AOPs, less HO$^\bullet$ exposure would be needed. Additionally, it is likely that the solar lamps would be cheaper and less energy-intensive than typical lamps used in AOPs, but this needs to be formally assessed.

In addition to the lamps, it would be prudent to investigate how to best configure disinfection contactors to maximize solution light absorbance and minimize reductions in FAC photolysis effectiveness due to water depth.

Overall, this research has demonstrated that photochemically activated FAC can enhance inactivation of chlorine-resistant microorganisms, *B. subtilis* spores. The enhanced inactivation effect was attributed to the generation of hydroxyl radical and was observed at different temperatures (10, 25, and 33°C), at a representative pH range: 6-8, with simulated and natural sunlight, and with phosphate-buffered solutions and natural water samples from drinking water treatment plants in the Seattle area. Given the observed enhancement benefits at each of these conditions, further research should investigate DBP formation and optimization of the method in

54

practice. In the future, the photochemical activation of FAC could be a promising method of drinking water treatment capable of removing chlorine-resistant pathogens in both temperate and tropical climates in centralized and decentralized settings.

5. REFERENCES

1. White, G.C.B.V. *White's Handbook of Chlorination and Alternative Disinfectants*. 5th Edition ed. 2010, New York, NY: John Wiley and Sons, Inc.
2. Water Chlorination/Chloramination Practices and Principles AWWA Manual M20, 2nd Edition, 2006.
3. Arnold, B. F.; Colford, J. M., Jr. Treating water with chlorine at point-of-use to improve water quality and reduce child diarrhea in developing countries: a systematic review and meta-analysis. *Am. J. Trop. Med. Hyg.* **2007**, *76* (2), 354–64.
4. Bystrianyk, R. Vital Statistics of the United States. 2001, HealthSentinel.com. Accessed 05/01/2012.
5. Mintz, E.; Reiff, F.; Tauxe, R. Safe water treatment and storage in the home: A practical new strategy to prevent waterborne disease. *JAMA* **1995**, 273: 948-953.
6. WHO, 2009. Death and Disability-adjusted Life Year (DALY) Rates, by WHO Region. World Health Organization.
7. EPA website, Basic Information about Disinfectants in Drinking Water: Chloramine, Chlorine and Chlorine Dioxide, http://water.epa.gov/drink/contaminants/basicinformation/disinfectants.cfm, accessed May 5, 2012.
8. World Health Organization, Guidelines for drinking-water quality, third edition, incorporating first and second addenda, Ch. 12: Chemical Factsheets, 2006.
9. Mackenzie, W. R., et al. A massive outbreak in milwaukee of *Cryptosporidium* infection transmitted through the public water-supply. *New Engl. J. Med.* **1994,** *331* (3), 161-167.
10. EPA, Water: Regulatory Information. http://water.epa.gov/lawsregs/rulesregs/ Accessed May 1, 2012.
11. *Community Water System Survey. Volume II: Detailed Tables and Survey Methodology*. United States Environmental Protection Agency: 2000.
12. Connick, R.E.; Chia, Y.T. The hydrolysis of chlorine and its variation with temperature. *Journal of the American Chemical Society,* **1959**. *81* (6), 1280-1284.
13. Sawyer, C.N.; McCarty, P.L.; Parkin, L.; Parkin, G.F. *Chemistry for Environmental Engineering;* 1994; McGraw Hill, Inc.: New York, NY.
14. Morris, J. C. Acid ionization constant of HOCl from 5 to 35 °. *J. Phys. Chem.* **1966,** *70* (12), 3798- 3805.
15. Atkin, E. W.; Hoff, J. C.; Lippy, E. C. Waterborne outbreak control: which disinfectant? *Environ. Health Perspect* **1982,** *46,* 7–12.
16. Lide, D. R., Ed. CRC Handbook of Chemistry and Physics, 2006, 86th ed.; Taylor & Francis Group: New York.
17. Carswell, J.K. et al. In J. Katz (ed.) *Ozone and chlorine dioxide technology for disinfection of drinking water.* 1980; Noyes Data Corporation: Park Ridge, NJ.
18. Schwarzenbach, R. P., Gschwend, P. M.; , Imboden, D. M., *Environmental Organic Chemistry*; 2nd ed. 2003; John Wiley &Sons, Inc.: Hoboken; p 658−666.
19. Venkobachar, C.; Iyengar, L.; Rao, A. V. S. P. Mechanism of Disinfection: Effect of Chlorine on Cell Membrane Functions. *Water Res.* **1977,** *11* (8), 727-729.

20. Haas, C. N.; Engelbrecht, R. S. Physiological alterations of vegetative microorganisms resulting from chlorination. *Journal of the Water Pollution Control Federation* **1980,** *52* (7), 1976-1989.

21. Young, S.B.; Setlow, P. Mechanisms of killing of *Bacilus subtilis* spores by hypochlorite and chlorine dioxide. *Journal of Appl. Microbiol.* **2003**, *95*, 54-67.

22. Hoff, J.C.; Rice, E.W.; Schaefer, F.W. Disinfection and the Control of Waterborne Giardiasis. Conference proceedings, ASCE Specialty Conference, 1984.

23. Taylor, R. H.; Falkinham III, J. O.; Norton, C. D.; LeChevallier, M. W. Chlorine, chloramine, chlorine dioxide, and ozone susceptibility of Mycobacterium avium. *Appl. Environ. Microbiol*. **2000**, *66*,1702–1705.

24. Fayer, R.; Speer, C.; Dubey, J. The General Biology of Cryptosporidium. In: Cryptosporidium and Cryptosporidiosis (Fayer, R. ed.). 1997; CRC Press: Boca Raton, New York, London, Tokyo, pp.1–42.

25. Rice, E.W.; Fox, K.R.; Miltner, R.J.; Lytle, D.A.; Johnson, C.H. Evaluating plant performance with endospores. *Journal of the American Water Works Association*, **1996,** *88* (9), 122-130.

26. Facile, N.; Barbeau, B.; Prévost, M.; Koudjonou, B. Evaluating bacterial aerobic spores as a surrogate for Giardia and Cryptosporidium inactivation by ozone. *Water Res.* **2000**, *34*, 3238–3246.

27. Owens, J.H.; Miltner, R.J.; Rice, E.W.; Johnson, C.H.; Dahling, D.R.; Schaefer, F.W.; Shukairy, H.M. Pilot-scale ozone inactivation of Cryptosporidium and other microorganisms in natural water. *Ozone: Sci. Eng.* **2000**, *22*, 501–517.

28. Craik, S.A. Smith, D.W., Belosevic, M. and M. Chandrakanth. Use of Bacillus subtilis spores as model micro- organisms for ozonation of Cryptosporidium parvum in drinking water treatment. *J. Environ. Eng. Sci.* **2002,** *1,* 173–186.

29. Barbeau, B.; Boulos, L.; Desjardins, R.; Coallier, J.; Prevost, M. Examining the use of aerobic spore-forming bacteria to assess the efficiency of chlorination. *Water Res*. **1999**, *33*, 2941–2948.

30. Riesenman, P.J.; Nicholson, W.L. Role of the Spore Coat Layers in Bacillus subtilis Spore Resistance to Hydrogen Peroxide, Artificial UV-C, UV-B, and Solar UV Radiation. *Appl. Environ. Microbiol*. **2000**, *66* (2), 620.

31. Setlow, P. Resistance of bacterial spores. In Bacterial Stress Responses ed. Storz, G. and Hengge-Aronis, R. 2000; American Society for Microbiology: Washington, DC, pp. 217–230.

32. Tennen, R.; Setlow, B.; Davis, K.L.; Loshon, C.A. Setlow, P. Mechanisms of killing of spores of Bacillus subtilis by iodine, glutaraldehyde and nitrous acid. *Journal of Appl. Microbiol.* **2000**, *89*, 330–338.

33. Setlow, B.; Setlow, P. Role of DNA repair in Bacillus subtilis spore resistance. *Journal of Bacteriol*., **1996**, *178*, 3486–3495.

34. Gong, A.S.; Lanzl, C.A.; Cwiertny, D.M.; Walker, S.L. Lack of Influence of Extracellular Polymeric Substances (EPS) Level on Hydroxyl Radical Mediated Disinfection of Escherichia coli. *Environ. Sci. Technol*. **2012**, *46*, 241–249.

35. Faust, B. C. In *Aquatic and Surface Photochemistry*; Helz, G. Zepp, R. G., Crosby, D. G., Eds. 1994; Lewis Publishers: Boca Raton; pp 3-3.

36. Vaughan, P. P.; Blough, N. V. Photochemical Formation of Hydroxyl Radical by Constituents of Natural Waters. *Environ. Sci. Technol*. **1998**, *32* (19), 2947–2953.

37. Nowell, L. H.; Hoigne, J. Photolysis of aqueous chlorine at sunlight and ultraviolet wavelengths - 2. Hydroxyl radical production. *Water Res.* **1992,** *26* (5), 599-605.

38. Nowell, L. H.; Hoigne, J. Photolysis of aqueous chlorine at sunlight and ultraviolet wavelengths - 1. Degradation rates. *Water Res.* **1992,** *26* (5), 593-598.

39. Mamane-Gravetz, H.; Linden, K.G.; Cabaj, A.; Sommer, R. Spectral sensitivity of *Bacillus subtilis* spores and MS2 coliphage for validation testing of water disinfection using ultraviolet reactors. *Environ. Sci. Technol.* **2005**, *39*, 7845–7852.

40. Cho, M.; Yoon, J. Enhanced bactericidal effect of O_3/H_2O_2 followed by Cl_2. *Ozone-Science & Engineering* **2006,** *28* (5), 335-340.

41. Alkan, U.; Teksoy, A.; Atesli, A.; Baskaya, H.S. Influence of humic substances on the UV disinfection of surface waters. *Water Environ. J.*, In Press.

42. von Sonntag, C. *The Chemical Basis of Radiation Biology*. 1987; Taylor and Francis: London, England.

43. von Sonntag, C. *Free-Radical-Induced DNA Damage and Its Repair: A Chemical Perspective*. Springer-Verlag: Berlin, Germany, 2006.

44. Buxton, G. V.; Greenstock, W. P.; Helman, W. P.; Ross, A. B. Critical review of rate constants for reactions of hydrated electrons, hydrogen atoms, and hydroxyl radicals (•OH/O•-) in aqueous solution. *J. Phys. Chem. Ref. Data* **1988,** *17*, 513-886.

45. Watts, M. J.; Linden, K. G. Chlorine photolysis and subsequent OH radical production during UV treatment of chlorinated water. *Water Res.* **2007,** *41* (13), 2871-2878.

46. Bolton J. R. and Cotton C. The Ultraviolet Disinfection Handbook. 2008; American Water Works Association.

47. SODIS- Safe Drinking Water for All. http://www.sodis.ch/index_EN, Accessed April 1, 2012.

48. Boyle, M. et al. Bactericidal Effect of Solar Water Disinfection under Real Sunlight Conditions. *Appl. and Env. Microbiol.* **2008**, *74* (10), 2997-3001.

49. Malato, S.; Fernandez-Ibanez, P.; Maldonado, M.I.; Blanco J.; Gernjak, W. Decontamination and disinfection of water by solar photocatalysis: Recent overview and trends. *Catalysis Today* **2009**, *147*:1-59.

50. Fisher, M.B.; Keenan, C.R.; Nelson, K.L.; Voelker, B.M. Speeding up solar disinfection (SODIS): effects of hydrogen peroxide, temperature, pH, and copper plus ascorbate on the photoinactivation of E. coli. *J. Water Health* **2008**, *6* (1), 35-51.

51. Amin, M.T.; Han, M. Roof-harvested rainwater for potable purposes: application of solar disinfection (SODIS) and limitations. *Water Science & Technol.* **2009**, *60*.

52. Chu, W. Modeling the quantum yields of herbicide 2,4-D decay in UV/H2O2 process. *Chemosphere* **2001,** *44*, 935–941.

53. Benitez, F.J.; Acero, A.J.; Real, F.J. Degradation of carbofuran by using ozone, UV radiation and advanced oxidation processes. *J. Hazard. Mater.* **2002,** *89*, 51–65.

54. Huber, M.M.; Canonica, S.; Park, G.Y.; von Gunten, U. Oxidation of phar-maceuticals during ozonation and advanced oxidation processes. *Environ. Sci. Technol.* **2003,** *37,* 1016–1024.

55. Zamy, C.; Mazellier, P.; Legube, B. Phototransformation of selected organophosphorus pesticides in dilute aqueous solutions. *Water Res.* **2004,** *38,* 2305–2314.

56. Shemer, H.; Kacar Kunukcu, Y.; Linden, K.G. Degradation of the pharmaceutical metronidazole via UV, Fenton, and photo-Fenton processes. *Chemosphere* **2006**, *63*, 269–276.

57. Rennecker, J. L.; Driedger, A. M.; Rubin, S. A.; Marinas, B. J. Synergy in sequential inactivation of *Cryptosporidium parvum* with ozone/free chlorine and ozone/monochloramine. *Water Res.* **2000,** *34* (17), 4121-4130.

58. Cho, M.; Gandhi, V.; Hwang, T. M.; Lee, S.; Kim, J. H. Investigating synergism during sequential inactivation of MS-2 phage and Bacillus subtilis spores with UV/H_2O_2 followed by free chlorine. *Water Res.* **2011,** *45* (3), 1063-1070.

59. Kumar, K.; Day, R. A.; Margerum, D. W. Atom-transfer redox kinetics: general-acid-assisted oxidation of iodide by chloramines and hypochlorite. *Inorg. Chem.* **1986**, *25*, 4344-4350.

60. APHA; AWWA; WEF. Standard Methods for the Examination of Water & Wastewater; American Public Health Association: Washington DC, 2005.

61. Molecular Cloning: A Laboratory Manual Vol. 3, J. Sambrook and D.W. Russell, 2001, Cold Spring Harbor Laboratory Press, Cold Spring Harbor, NY.

62. Beck, N. K.; Callahan, K.; Nappier, S. P.; Kim, H.; Sobsey, M. D.; Meschke, J. S. Development of a spot-titer culture assay for quantifying bacteria and viral indicators. *J. Rapid Methods Autom. Microbiol.* **2009,** *17* (4), 455-464.

63. Dulin, D.; Mill, T. Development and evaluation of sunlight actinometers. *Environ. Sci. Technol.* **1982,** *16* (11), 815-820.

64. Cho, M.; Lee, Y.; Chung, H.; Yoon, J. Inactivation of Escherichia coli by photochemical reaction of ferrioxalate at slightly acidic and near-neutral pHs. *Appl. Environ. Microbiol.* **2004,** *70* (2), 1129- 1134.

65. Rennecker, J. L.; Marinas, B. J.; Owens, J. H.; Rice E. W. Inactivation of *Cryptosporidium parvum* oocysts with ozone. *Water Res.* **1999**, *31* (11), 2481-2488.

66. Elovitz, M. S.; von Gunten, U. Hydroxyl radical/ozone ratios during ozonation processes. I. The *Rct* concept. *Ozone-Science & Engineering* **1999**, *21* (3), 239-260.

67. Rosenfeldt, E. J.; Linden, K. G. The R•OH,UV concept to characterize and the model UV/H_2O_2 process in natural waters. *Environ. Sci. Technol.* **2007,** *41* (7), 2548-2553.

68. Weishaar, J.L.; Aiken, G.r.; Beramaschi, B.A.; Fram, M.S.; Fujii, R.; Moper, K. Evaluation of Specific Ultraviolet Absorbance as an Indicator of the Chemical Composition and Reactivity of Dissolved Organic Carbon. *Environ. Sci. Technol.* **2003**, *37,* 4702-4708.

69. Li, H.; Finch, G.R.; Smith, D.W.; Belosevic, M. Sequential inactivation of *Cryptosporidium parvum* using ozone and chlorine. *Water Res.* **2001**, *35,* (18), 4339–4348.

70. Sagripanti, JL; Bonifacino, A. Comparative sporicidal effects of liquid chemical agents. *Applied and Environmental Microbiology* **1996**, *62* (2), 545-551.

71. Dong, M. M.; Mezyk, S. P.; Rosario-Ortiz, F. L. Reactivity of effluent organic matter (Ef0M) with hydroxyl radical as a function of molecular weight. *Environ. Sci. Technol.* **2010**, 44 (15), 5714–5720.

72. Rosario-Ortiz, F. L.; Mezyk, S. P.; Doud, D. F. R.; Snyder, S. A. Quantitative correlation of absolute hydroxyl radical rate constants with mon-isolated effluent organic matter bulk properties in water. *Environ. Sci. Technol.* **2008**, 42 (16), 5924–5930.

73. Westerhoff, P.; Aiken, G.; Amy, G.; Debroux, J. Relationships between the structure of natural organic matter and its reactivity towards molecular ozone and hydroxyl radicals. *Water Res*. **1999**, *33* (10), 2265–2276.

74. Rincón, A.G.; Pulgarin, C.; Adler, N.; Peringer, P. Interaction between *E. coli* inactivation and DBP - precursors- dihydroxybenzene isomers- in the photocatalytic process of drinking-water disinfection with TiO$_2$. *J. Photochem. Photobiol. A: Chem.* **2001**, *139*, 233–241.

75. Cho, M.; Chung, H. M.; Yoon, J. Disinfection of water containing natural organic matter by using ozone-initiated radical reactions. *Appl. Environ. Microbiol.* **2003,** *69* (4), 2284-2291.

76. Barbeau, B.; Rivard, M.; Prevos, M. The impact of natural organic matter on free chiorine and chlorine dioxide disinfection efficacy *Journal of Water Supply: Research and Technology* **2006**, 383-390.

77. Koshikawa, T.; Yamazaki, M.; Yoshimi, M.; Ogawa, S.; Yamada, A.; Watabe, K.; Tori, M. Surface Hydrophobicity of Spores of Bacillus spp. *Journal of General Microbiol.* **1989**, *135*, 2717-2722.

78. von Gunten, U.; Oliveras, Y. Advanced oxidation of bromide-containing waters: Bromate formation mechanisms. *Environ. Sci. Technol.* **1998,** *32* (1), 63-70.

79. von Gunten, U. Ozonation of drinking water: Part I. Oxidation kinetics and product formation. *Water Res.* **2003,** *37*, 1443-1467.

80. Siddiqui, M.S., Chlorine-ozone interactions: formation of chlorate. *Water Research* **1996,** 30 (9), 2160-2170.

81. Munichandraiah, N., Sathyanarayana, S., 1987. Kinetics and mechanism of anodic oxidation of chlorate ion to perchlorate ion on lead dioxide electrodes. *Journal of Appl. Electrochemistry* **1987,** 17, 33-48.

82. von Gunten, U.; Driedger, A.; Gallard, H.; Salhi, E. By-prodcuts formation during drinking water disinfection: a tool to assess disinfection efficiency. *Water Res* **2001**, *35*, 2095–2099.

83. Kimball, A.W. The fitting of multi-hit survival curves. *Biometrics*, **1953**, *9*, 201–211.

84. Nicholson, W.L.; Munakata, N.; Horneck, G.; Melosh, H.J.; Setlow, P. Resistance of Bacillus Endospores to Extreme Terrestrial and Extraterrestrial Environments. *Microbiology and Molecular Biology Reviews*, **2000**, *64* (3), 548–572.

85. Cross, J. B.; Currier, R. P.; Torraco, D. J.; Vanderberg, L. A.; Wagner, G. L.; Gladen, P.D. Killing of Bacillus Spores by Aqueous Dissolved Oxygen, Ascorbic Acid, and Copper Ions. *Appl. Environ. Microbiol*. **2003**, *69* (4): 2245-2252.

86. Driks, A. *Bacillus subtilis* spore coat. *Molecular Biol. and Microbiol. Reviews* **1999**, *63*, 1–20.

87. Cho, M.; Yoon, J. Measurement of OH radical CT for inactivating Cryptosporidium parvum using photo/ferrioxalate and photo/TiO2 systems. *J. Appl. Microbiol.* **2008,** *104* (3), 759-766.